Molecular Pharmacology Fast Forward. Published on April 10, 2014 as doi:10.1124/mol.113.090183

MOL # 90183

Title Page

Structure, molecular modeling and function of a novel potassium channel blocker, urotoxin, isolated from the venom of the Australian scorpion *Urodacus yaschenkoi*

Karen Luna-Ramírez, Adam Bartok, Rita Restano-Cassulini, Veronica Quintero-Hernández, Fredy I.V. Coronas, Janni Christensen, Christine E. Wright, Gyorgy Panyi and Lourival D. Possani

Australian Venom Research Unit and Cardiovascular Therapeutics Unit, Department of Pharmacology and Therapeutics, University of Melbourne, Parkville, Victoria 3010, Australia (KLR and CEW)

Departamento de Medicina Molecular y Bioprocesos, Instituto de Biotecnología, Universidad Nacional Autónoma de México, Avenida Universidad, 2001, Colonia Chamilpa, Apartado Postal 510-3, Cuernavaca 62210, México (RRC, VQH, FIVC, LDP)

Department of Biophysics and Cell Biology, Research Center for Molecular Medicine, University of Debrecen, 98 Nagyerdei krt, Debrecen, 4032, Hungary (AB and GP)

MTA-DE Cell Biology and Signaling Research Group, Egyetem tér 1, Debrecen, 4032, Hungary (GP).

Department of Biochemistry, La Trobe Institute for Molecular Science, La Trobe University, Melbourne, Victoria 3086, Australia (JC)

Molecular Pharmacology Fast Forward. Published on April 10, 2014 as DOI: 10.1124/mol.113.090183
This article has not been copyedited and formatted. The final version may differ from this version.

Running Title page

Running title: Characterization of the potassium channel blocker urotoxin

Corresponding authors:

i) Karen Luna-Ramírez, AVRU and CTU, Department of Pharmacology and Therapeutics, University of Melbourne, Parkville, Victoria 3010, Australia. Email: karenlr@student.unimelb.edu.au, Phone: +61 3 8344 8219

ii) Lourival D. Possani, Institute of Biotechnology, UNAM, Avenida Universidad, 2001, Apartado Postal 510-3 Cuernavaca Morelos 62210 México. Email: possani@ibt.unam.mx, Phone: +52-77-73171209

Number of text pages: 22;

Tables: 2;

Figures: 9;

References: 52.

Abstract: 246 words

Introduction: 672 words

Discussion: 1500 words

List of nonstandard abbreviations

Abbreviation	**Meaning**
α-KTx	Alpha-potassium channel toxin
ChTx	Charybdotoxin
ESI	Electro spray ionization
Kv	voltage-gated potassium channel
MD	Molecular dynamics
NGS	Next generation sequencing
O. carinatus	*Opistophthalmus carinatus*

Molecular Pharmacology Fast Forward. Published on April 10, 2014 as DOI: 10.1124/mol.113.090183
This article has not been copyedited and formatted. The final version may differ from this version.

Abstract

This communication reports the structural and functional characterization of urotoxin, the first K^+ channel toxin isolated from the venom of the Australian scorpion *Urodacus yaschenkoi*. It is a basic peptide consisting of 37 amino acids with an amidated C-terminal residue. Urotoxin contains 8 cysteines forming 4 disulfide bridges with sequence similarities resembling the α-KTx-6 subfamily of peptides; it was assigned the systematic number of α-KTx-6.21. Urotoxin is a potent blocker of human Kv1.2 channels, with an IC_{50} of 160 pM, whereas its affinity for other channels tested was in the nanomolar range (hKv1.1, IC_{50} = 253 nM; hKv1.3, IC_{50} = 91 nM; and hKCa3.1, IC_{50} = 70 nM). The toxin had no effect on hKv1.4, hKv1.5, hERG1 and hELK2 channels. Multiple sequence alignments from the venom gland transcriptome showed the existence of four other new peptides similar to urotoxin. Computer modeling of urotoxin's 3D structure suggests the presence of the α/β-scaffold characteristic of other scorpion toxins, although very likely forming an uncommon disulfide pairing pattern. Using molecular dynamics, a model for the binding of this peptide to human Kv1.2 and hKv1.1 channels is presented, along with the binding of an *in silico* mutant urotoxin (Lys25Ala) to both channels. Urotoxin enriches our knowledge of K^+ channel toxins and due to its high affinity for hKv1.2 channels, it may be a good candidate for the development of pharmacological tools to study the physiological functions of K^+ channels or related channelopathies and for restoring axonal conduction in demyelinated axons.

Molecular Pharmacology Fast Forward. Published on April 10, 2014 as DOI: 10.1124/mol.113.090183
This article has not been copyedited and formatted. The final version may differ from this version.

1. Introduction

Scorpion venoms provide a rich source of neurotoxins that bind to ion channels. These toxins have proven to be excellent tools for the identification and classification of Na^+, K^+, $Ca^{2+}$and Cl^- channels and their families and subfamilies, for the characterization of the tissue distribution of the ion channels and for the understanding of the role of ion channels in certain types of pathologies [reviewed in (Possani et al., 1999), (Gati et al., 2012)].

Potassium channels are ubiquitous membrane proteins found in both excitable and non-excitable cells (Shieh et al., 2000). Ninety-two K^+ channel genes have been identified in the human genome (http://www.genenames.org/genefamilies/KCN) which makes K^+ channels the most diverse of all ion channel families regarding primary structure and physiological function. They are involved in the regulation of various cellular processes including cell proliferation (Wonderlin and Strobl, 1996), apoptosis (Burg et al., 2006), hormone secretion, K^+ homeostasis, neurotransmitter release and modulation of the action potential (Bauer and Schwarz, 2001). Consequently, changes in the activity of K^+ channels due to K^+ channel gene mutations, drug actions and/or regulation of channel functions by hormones and neurotransmitters lead to diseases of the central nervous system, heart, kidney and pancreas (Restrepo-Angulo et al., 2010; Shieh et al., 2000).

Toxins that block K^+ channels are minor components of a scorpion venom, however, they are also found in venoms of other organisms (Legros et al., 1996). Based on to the alignment of the cysteine residues and other highly conserved amino acids, the K^+ channel-blocking scorpion toxins have been classified into four families: α-KTx, β-KTx, γ-KTx, and κ-KTx (Rodríguez de la Vega and Possani, 2004; Tytgat et al., 1999). The α-KTx is the best-studied family; its members are small basic peptides (up to 4 KDa) consisting of 23-40 amino acids with the structure stabilized by three to four disulfide bridges. To date, the α-KTx family is classified into 27 subfamilies (http://www.uniprot.org/docs/scorpktx) (Goudet et al., 2002; Gurrola et al., 2012; Huys et al., 2004; Rodríguez de la Vega and Possani, 2004; Tan et al., 2006; Tytgat et al., 1999; Zhijian et al., 2006) with K^+ channel affinities varying in the micromolar to picomolar range. α-KTx toxins target mainly the voltage-gated potassium (Kv) channels, especially the Kv1 family members and some Ca^{2+}-

Molecular Pharmacology Fast Forward. Published on April 10, 2014 as DOI: 10.1124/mol.113.090183
This article has not been copyedited and formatted. The final version may differ from this version.

activated K^+ channels (Rodríguez de la Vega and Possani, 2004; Tytgat et al., 1999). α-KTx toxin structures are similar and their specificity and affinity depend on the amino acid side chains situated on the external surface and those pointing towards the contact surface with the channel (Jouirou et al., 2004; Rodríguez de la Vega et al., 2003). There are currently 131 known α-K^+-channel toxins from scorpion venom (Martin-Eauclaire and Bougis, 2012, http://www.uniprot.org/docs/scorpktx).

This work describes the first K^+-channel toxin from an Urodacidae scorpion. The peptide was isolated from the venom of the *Urodacus yaschenkoi* scorpion and its primary structure was determined by automatic Edman degradation and nucleotide sequencing, using a Next Generation Sequencing approach. The peptide is a very potent blocker of the hKv1.2 channel, although it also inhibits hKv1.1, hKv1.3 and hKCa3.1 channels with lower potency, but does not block other channels included in this study (hKv1.4, hKv1.5, hERG1 and hELK2). The computer-modeled (MAESTRO software) 3D structure of the toxin revealed an α/β-scaffold characteristic of the α-KTx scorpion toxins. Molecular dynamics simulation showed that the interaction of urotoxin with hKv1.2 relies on the hydrogen bonds between lysines and an arginine on the peptide and acidic residues in the turret and the pore helix of the channel. Additionally, a simulation with mutant-urotoxin (Lys25Ala) indicated that Lys25 does not have the same role in the binding of urotoxin to hKv1.2 as in other α-KTx-6 toxins. Our results suggest that urotoxin may be useful as a pharmacological tool to reveal the physiological function of hKv1.2 channels in *in vitro* and *in vivo* experiments, a lead for peptidomimetics for the targeting of hKv1.2 channels, and may be an experimental therapeutic tool to restore axonal conduction in demyelinated axons, where inhibition of K^+ channels has beneficial effects (Beraud et al., 2006; Shi and Sun, 2011).

Molecular Pharmacology Fast Forward. Published on April 10, 2014 as DOI: 10.1124/mol.113.090183
This article has not been copyedited and formatted. The final version may differ from this version.

2. Materials and Methods

2.1 Specimen collection and venom extraction

U. yaschenkoi scorpions were collected in the semi-arid and arid regions of Australia (near Broken Hill, NSW) by setting pitfalls along red sand dunes. The captured animals were maintained in plastic boxes with water *ad libitum* and were fed fortnightly with crickets.

Venom was obtained in the laboratory by electrical stimulation in the articulation of the telson as previously described (Luna-Ramírez et al., 2013). The venom was collected in Eppendorf Lo-bind™ tubes, and then centrifuged at 14000 *g* for 15 min at 4°C. The supernatant was pooled and finally freeze-dried and stored at -20°C until use. The protein concentration was determined by spectrophotometer Nanodrop® (Thermo Scientific) using the default program for proteins at λ=280 nm.

2.2 Venom separation

Initially, the soluble *U. yaschenkoi* venom was separated by reverse phase high performance liquid chromatography (RP-HPLC). The stored venom was solubilized in water and spun at 10,000 *g* for 5 min. One hundred microliters containing 3.0 mg of the soluble venom was directly submitted to an analytical C18 reversed phase column (250 mm × 10 mm) obtained from Vydac (Hisperia, CA, USA). Elution of the venom was made with a linear gradient of solution A [0.12% trifluoroacetic acid (TFA) in water] to 60% solution B (0.10% TFA in acetonitrile), run for 60 min, using a Waters 625 LC System coupled with a Waters 996 Photodiode Array Detector at 230 nm of absorbance with 0.5 U sensitivity and eluted at 1 ml/min flow-rate. Fractions were collected manually every 5 min and finally freeze-dried using a Speed-Vac Savant drier from ThermoFisher Co (San Jose, CA, USA).

Based on our previous work (Luna-Ramírez et al., 2013), the fractions containing mainly components with molecular weight ranging from 4-7 KDa were assayed for their K^+ channels inhibition properties, using cellular electrophysiology (patch-clamp technique). The effect of fractions 4 and 5 corresponding to retention times (RT) of 15:56-20:36 and 20:37-24:80 (Fig. 1) were screened against

Molecular Pharmacology Fast Forward. Published on April 10, 2014 as DOI: 10.1124/mol.113.090183
This article has not been copyedited and formatted. The final version may differ from this version.

4 potassium channels expressed heterologously: hKv1.1, hKv1.4, hERG1 (hKv11.1) and hELK2 (hKv12.2). Since Fraction 4 contained a putative K^+ channel-blocking peptide, was further purified (as described below) and screened against 8 K^+ channels.

2.3 Repurification of active fraction

Fraction 4 was re-purified using RP-HPLC with a linear gradient of 5-30% of solution B (0.10% TFA in acetonitrile), run for 60 min using the same conditions as described above. Each peak was collected manually and then assayed once more for the K^+ channel blocking potency using patch-clamp. This strategy permitted the selection of highly purified peptides for further characterization concerning molecular weight and sequence determination.

2.4 Amino acid sequence determination and mass spectrometry analysis

Amino acid sequence determination of the N-terminal segment of the purified peptide was obtained by automatic Edman degradation into a protein sequencer PPSQ-31A SHIMADZU (Kyoto, Japan) using the chemicals and procedures recommended by the provider.

Molecular weight determination of pure urotoxin was performed by LC-ESI- IT/MS with a Thermo Electron/Finningan LCQ Ion Trap Mass spectrometer (San Jose CA, USA). The sample (0.1-0.5 μg/μl) was dissolved in 50% acetonitrile with 0.1% acetic acid and directly applied into the LC-MS system as described earlier by our group (Batista et al., 2007).

2.5 Sequence elucidation by whole transcriptome using Next Generation Sequencing-Illumina

An mRNA-Seq library was generated from the venom gland of a carefully identified specimen of *U. yaschenkoi* according to Illumina's sample preparation instructions (TruSeqTM RNA Sample Preparation Guide). The purified cDNA library was used for cluster generation on Illumina's Cluster Station and then sequenced on Illumina HiSeq^{TM} 2000 following vendor's instructions. Typically, a paired-end sequencing run with a 101 nucleotides (nt) read length was used. For each run, RNA-Seq read was performed. Raw sequencing intensities were then extracted and the bases were called using Illumina's RTA software, followed by sequence quality filtering. The extracted sequencing reads were saved as a pair of fastq files for the first and second read, respectively. All raw reads generated from

Molecular Pharmacology Fast Forward. Published on April 10, 2014 as DOI: 10.1124/mol.113.090183
This article has not been copyedited and formatted. The final version may differ from this version.

the sequencer were *de novo* assembled into contigs using the Trinity program (Grabherr et al., 2011). The information concerning proteins of scorpions was collected from the NCBI non-redundant (nr) database. These annotated proteins were aligned to the assembled contigs to identify the homologous genes in *Urodacus yaschenkoi* using TBLASTN (E-value < 0.1). The nucleotide sequence of urotoxin was obtained from this library by comparison with the amino acid sequence obtained by Edman degradation and the theoretical molecular weight of this sequence with that directly measured by mass spectrometry.

2.6 Electrophysiology

2.6.1. Cell culture

Cell lines were cultured in Dulbecco's Modified Eagle Medium (DMEM) supplemented with 10% fetal bovine serum and maintained at 37°C in 5% CO_2 atmosphere and 95% humidity atmosphere. Transient expression of hKv1.1 and hKv1.4: CHO cells were co-transfected with plasmids of interest along with plasmid for green fluorescent protein (GFP) by using LipoFectamine (Life Technologies Corporation). Transient expression of hKv1.2: Cos7 cells were transfected with pCMV6 vector containing the GFP-tagged hKv1.2 gene (OriGene Technologies, Rockville, MD) using Lipofectamine 2000 reagent (Life Technologies Corporation). HEK tsA201 cells were transiently transfected with the hKCa3.1 gene in pEGFP-C1 (gift of Dr. Heike Wulff, University of California, Davis, CA) or with the hKv1.5 gene in pYFP-C1 plasmid (gift of Dr. Antonio Felipe, University of Barcelona, Barcelona, Spain) using Lipofectamine 2000. Cells were cultured under standard conditions. Currents were measured 1-2 days after transfection.

hERG1 and hELK2 channels were stably expressed in CHO and HEK cells, respectively (Redaelli et al., 2010). The hKv1.1, hKv1.4, hERG1 plasmids and hELK2 cell line were a gift from E. Wanke, Universitá di Milano Bicocca, Italy.

Kv1.3 currents were measured in human peripheral T lymphocytes isolated from healthy male volunteers. Mononuclear cells were separated by Ficoll-Hypaque density gradient centrifugation. Collected cells were washed twice with Ca^{2+}- and Mg^{2+}-free Hanks' solution containing 25 mM HEPES buffer, pH 7.4. Cells were cultured in a 5% CO_2 incubator at 37°C in 24-well culture plates in

Molecular Pharmacology Fast Forward. Published on April 10, 2014 as DOI: 10.1124/mol.113.090183
This article has not been copyedited and formatted. The final version may differ from this version.

RPMI 1640 medium supplemented with 10% fetal calf serum, 100 μg/ml penicillin, 100 μg/ml streptomycin, and 2 mM l-glutamine at 0.5×10^6/ml density for 2 to 6 days. Lymphocytes were activated with 2.5, 5 or 10 μg/ml phytohemagglutinin A (Sigma-Aldrich Kft, Budapest, Hungary) in the culturing medium.

2.6.2. Solutions

For recording hKv1.1and hKv1.4 currents, the standard extracellular solution contained (mM): NaCl 130, KCl 5, $CaCl_2$ 2, $MgCl_2$ 2, HEPES 10, d-glucose 5, pH 7.40 whereas the pipette solution contained (in mM): K^+-aspartate 130, NaCl 10, $MgCl_2$ 2, EGTA-KOH 10, HEPES-KOH 10 at pH 7.3 and nominal free Ca^{2+} concentration of 50 nM (Redaelli et al., 2010). For recording hKv1.2, hKv1.3, hKv1.5 and hKCa3.1 the extracellular (bath) solution contained (in mM): 145 NaCl, 5 KCl, 1 $MgCl_2$, 2.5 $CaCl_2$, 5.5 glucose, 10 HEPES, and 0.1 mg/ml BSA pH = 7.35. For the recordings of hKv1.2, hKv1.3 and hKv1.5 currents, the pipette-filling solution contained (in mM) 140 KF, 2 $MgCl_2$, 1 $CaCl_2$, 10 HEPES and 11 EGTA, pH = 7.2; whereas for the recording of hKCa3.1 currents it contained 150 K-aspartate, 5 HEPES, 10 EGTA, 8.7 $CaCl_2$, 2 $MgCl_2$, (pH 7.2). This latter pipette-filling solution contained 1 μM free Ca^{2+} concentration to fully activate the KCa3.1 current (Grissmer et al., 1993).

hERG1 and hELK2 currents were recorded in a high K^+ extracellular solution ($[K^+]_o$ = 40 mM) where NaCl was replaced by an equimolar amount of KCl and using the K^+-aspartate-based pipette-filling solution (see above). This experimental condition provided the best signal-to-noise relation for hERG1 and hELK2 channels. Due to the low amount of material in Fraction 4 of the venom the high K^+ extracellular solution was also used to analyze the effect of the venom fractions on the hKv1.1 and hKv1.4 currents. Toxin fractions from concentrated stocks in distilled water were diluted directly into the extracellular solution. Osmolarity of the extracellular solution was between 302 and 308 mOsm and that of the intracellular solutions were ~295 mOsm.

2.6.3. Patch-clamp recordings and data analysis

Currents were measured using whole-cell or outside-out patch configuration in voltage clamp mode using Axopatch 200A and MultiClamp 700B amplifiers and Digidata 1200/1440A digitizers. For data analysis the pClamp9/10 software package was used. For recording of hKv1.2, hKv1.3 and hKv1.5

Molecular Pharmacology Fast Forward. Published on April 10, 2014 as DOI: 10.1124/mol.113.090183
This article has not been copyedited and formatted. The final version may differ from this version.

currents, the cells were held at −100 mV holding potential and depolarized to +50 mV for 15 ms (hKv1.3) or 200 ms (hKv1.2) or 40 ms (hKv1.5) every 15 s to fully activate the currents. For recording of hKv1.1 and hKv1.4 currents cells were held at −90 mV holding potential and depolarized at +60 mV for 200 or 300 ms followed by a repolarizing step at −50 mV (100 ms). Time between pulses was 2.7 s. For recording of hERG1 tail currents, the cells were held at −80 mV, depolarized at +60 mV for 500 ms to activate the current and the membrane potential was stepped back at −120 mV to record the inward tail current, pulses were delivered every 5 s. hELK2 currents were evoked by voltage steps to −120 mV for 500 ms from a holding potential of +30 mV. hKCa3.1 currents were evoked by 150-ms-long voltage ramps from −120 to +40 mV every 10 s from a holding potential of −100 mV.

Micropipettes were pulled from GC 150 F-15 borosilicate capillaries with a resistance of 3-5 MΩ in the bath solution. When necessary, 80-90% of cell capacitance and series resistance errors were compensated for before each voltage clamp protocol in order to decrease the voltage errors to less than 5% of the protocol pulse. The effect of the toxin in a given concentration is displayed as remaining current fraction ($RF= I/I_0$, where I is the current amplitude measured in the presence of the toxin upon reaching block equilibrium, I_0 is the current amplitude measured in the toxin-free control bath solution). Data points of the concentration-response curves are averages of 3-5 independent measurements where the error bars represent the S.E.M. The two parameter Hill equation was fitted on the points ($RF = IC_{50}^{H}/(IC_{50}^{H}+[Tx]^{H})$, where IC_{50} is the half-maximum inhibition dose, H is the Hill coefficient and [Tx] is the toxin concentration. The limited amount of natural urotoxin did not allow determination of the IC_{50} in the nanomolar range for Kv1.3 and KCa3.1, therefore, we used the Lineweaver-Burk analysis, where 1/RF calculated from 3-5 independent measurements was plotted as a function of toxin concentration and a straight line was fitted to the points, where IC_{50} = 1/slope.

2.7 Modeling

2.7.1. Homology model of urotoxin

The primary structure of urotoxin shares high sequence similarity with α-KTx-6 family members containing the Toxin 2 superfamily region (according to BlastP) and the 8 cysteines binding motif. To

Molecular Pharmacology Fast Forward. Published on April 10, 2014 as DOI: 10.1124/mol.113.090183
This article has not been copyedited and formatted. The final version may differ from this version.

model its 3-D structure, we used a template based on the most similar toxin to urotoxin that has a crystal or solution NMR structure. A search for similar sequences using the BLAST program against the Protein Data Bank Proteins (PDB) database revealed 57.9% identity with the sequence of spinoxin (PDB = 1V56), whose three-dimensional structure has been solved. The homology model was made with MAESTRO software (Maestro, version 9.3, Schrödinger, LLC, New York, NY, 2012) and the amidation of the last residue was made using VMD psfgen.

2.7.2 Molecular dynamics simulation of urotoxin binding to hKv1.1 and hKv1.2 channels

Homology models of the pore domains of hKv1.1 and hKv1.2 channels from crystal structure of rat Kv1.2 (PDB 3LUT) (Chen et al., 2010) were constructed using the methods of Chen et al. (2011). For hKv1.1, sequence gi|119395748 was used and for hKv1.2 gi|4826782. Molecular dynamics simulation of urotoxin binding to the hKv1.1 and hKv1.2 homology models was made using Maestro software in the super computer AVOCA (IBM Blue Gene/Q; University of Melbourne). Channel-toxin complexes were refined with MD simulations in order to identify the interacting residues of urotoxin with hKv1.1 and hKv1.2 channels. Each channel was embedded in a 1-palmitoyl-2-oleoyl-sn-glycero-3-phosphocholine (POPC) bilayer (≈80 lipids/leaflet) and a box of explicit TIP3P water (≈87,000 molecules). Approximately 12 K^+, 88 Cl^- and 74 Na^+ ions were added giving an overall cation concentration of 0.2 M. First, the system was equilibrated for 25 ns where the C-alpha atoms in the toxin and the whole channel were kept rigid to ensure that the membrane had good contact with the protein channel. Subsequently a 5 ns equilibration with no restraints was performed. Finally two sets of 10 x 50 ns brute force molecular dynamics simulations were performed at 310 K using NAMD v2.9. Recognition residues and interaction contacts for the binding were identified during this time of simulation. The CHARMM27 force field was used. Visualizations of molecules are in VMD software.

2.7.3 In silico generation of the Lys25Ala mutant urotoxin and MD simulation

Residue lysine-25 was mutated *in silico* to alanine (Lys25Ala) with the Mutator plug-in from VMD and the 500 ns brute force dynamics simulation was performed as described in Section 2.7.2.

Molecular Pharmacology Fast Forward. Published on April 10, 2014 as DOI: 10.1124/mol.113.090183
This article has not been copyedited and formatted. The final version may differ from this version.

3. Results

3.1. Isolation of urotoxin and molecular weight determination

A sample containing 3.0 mg of protein from the soluble venom of the scorpion *U. yaschenkoi* was routinely separated by HPLC as previously shown (Luna-Ramírez et al., 2013). The fraction collection from the HPLC was performed every 5 min of elution time in order to reduce the number of fractions to be screened in electrophysiology Fig. 1 shows the HPLC separation of the soluble venom, where the peak at minute 18 (within Fraction 4) indicates the elution of the peptide described below. The main component of Fraction 4 (labeled with an arrow) was collected separately and finally obtained in pure form (see Fig.1 inset), using a gradient of 5-30% solution B [0.10% TFA in acetonitrile]), over 60 min. The major component eluted at 27.3 min. (labeled in the inset with an asterisk) was homogeneous and shown by ESI-MS spectrometry to contain a peptide with molecular mass of 4012.75 Da corresponding adequately to the mass fingerprinting made previously by our group (Luna-Ramírez et al., 2013). This peptide is referred to as urotoxin throughout the paper.

3.2 Sequence elucidation

Urotoxin was sequenced by automatic Edman degradation giving a partial N-terminal amino acid sequence from residues number 1 up to 19 (GDIKXSGTRQXWGPXKKQT). Since the peptide was not previously reduced and alkylated for Edman degradation, the X residues were assumed to be cysteines; which was later confirmed using nucleotide sequence analysis. Using Next Generation Sequencing (NGS) analysis the full sequence of this toxin was unveiled (Supplemental Figure 1). From the NGS study, four additional new peptides similar to urotoxin were detected (isotigs) which may be isoforms or *bona fide* similar peptides present in the venom. Alternatively, different genes may encode the same peptide, which has to be confirmed *a posteriori*. These five similar transcripts were analyzed as previously described (Luna-Ramírez et al., 2013) to obtain the mature peptide (Fig. 2). Briefly, with the sequences provided by NGS analysis having hits with K^+ channel toxins, the Expasy Translate tool was used to find the open reading frame; later Blastp was used to confirm that the translated sequence shares homology with K^+ channel toxins and finally, the mature peptide was found with SignalP.

Molecular Pharmacology Fast Forward. Published on April 10, 2014 as DOI: 10.1124/mol.113.090183
This article has not been copyedited and formatted. The final version may differ from this version.

The experimental molecular weight determined by mass spectrometry of the purified peptide, showed a molecular mass of 4012.75 Da. The translated sequence gave a theoretical expected molecular weight of 4070.7 Da for the folded peptide, meaning there was a difference of 57.95 Da, which corresponds to the molecular mass of glycine. This is consistent with the C-terminal amidation of urotoxin. According to the known processes that occur during expression of scorpion toxins (Becerril et al., 1993), the last residue of the peptide (glycine) is eliminated during the process of maturation and the amino group of the glycine is used for amidation of the previous residue (resulting in this case in valinamide). Thus, we conclude that the complete amino acid sequence of mature urotoxin is GDIKCSGTRQCWGPCKKQTTCTNSKCMNGKCKCYGCV*(G), where * means that valine (V) is amidated. The sequence analysis indicates that urotoxin belongs to the α-KTX-6 subfamily. Toxins from this subfamily share important features in their primary structure such as a central lysine (K25 or K23 in other toxins) that is critical for inhibition of Shaker channels, an essential dyad KC-N at positions 25-28 and the presence of eight conserved cysteines to stabilize the 3D structure of the toxins by disulfide bonds.

3.3 Pharmacological effects of urotoxin

The *in vitro* pharmacological effects of urotoxin were determined on eight K^+ channels using electrophysiology. Among these, five channels were members of the voltage-gated Shaker family (hKv1.1, hKv1.2, hKv1.3, hKv1.4 and hKv1.5), other channels included in the study were hERG1 and hELK2 and the intermediate conductance calcium-activated potassium channel, hKCa3.1. The initial assays were conducted using 10 nM toxin concentrations. When positive results were found, additional concentrations were assayed ideally up to 1 μM. Lack of available material limited the use of higher concentrations in several assays, as well as the broadening of the selectivity studies over a wider range of ion channels.

First, Fraction 4 (elution time 15 to 20 min of Fig. 1) was tested against hKv1.1, hKv1.4, hERG1 and hELK2. Fig. 3 shows the electrophysiological recordings obtained upon application of 50 μg/ml protein to hKv1.1, hKv1.4, hERG1 and hELK2 channels. Since Fraction 4 contains several components we cannot specify the exact molar concentration used. This fraction induced an almost

Molecular Pharmacology Fast Forward. Published on April 10, 2014 as DOI: 10.1124/mol.113.090183
This article has not been copyedited and formatted. The final version may differ from this version.

complete inhibition of the hKv1.1 current, whereas no effect was observed at identical toxin concentrations on other potassium channel types included in the screening (Fig. 3).

Upon purification of urotoxin to homogeneity (Fig. 1), it was assayed against hKv1.1, hKv1.2, hKv1.3, hKv1.5 and hKCa3.1 channels to provide more information about its selectivity. Electrophysiological recordings in Fig. 4A show that 1 μM of pure urotoxin inhibited hKv1.1 channels. The concentration-response curve (remaining current fraction recorded after application of different toxin concentrations) is plotted in Fig. 4B, where the solid line is the best fit resulting in an IC_{50} and Hill coefficient (H) of 253 nM and 1.1, respectively. The inhibition of the hKv1.1 current in the presence of 1 μM urotoxin was fast and reversible (Fig. 4C).

As the hKv1.1 channel is closely related to hKv1.2 and hKv1.3 (Robbins and Tempel, 2012; Wang et al., 1994; Xie et al., 2010), urotoxin was additionally tested in the latter two channels. Urotoxin, at 10 nM, fully blocked the whole cell hKv1.2 current (Fig. 5A), and the block was fully reversible when the recording chamber was washed using toxin-free solution (Fig. 5C). The concentration-response relationship of the block of hKv1.2 channels gave an IC_{50} of 160 pM (H= 1.1) (Fig. 5E). Figs. 5B and D show that 10 nM urotoxin quickly and reversibly inhibits the hKv1.3 current with an IC_{50} of 91 nM (Fig. 5F). These data mean that urotoxin is ~560-fold selective for hKv1.2 over hKv1.3 and ~1600-fold when compared to hKv1.1. Based on the classification of Giangiacomo and colleagues (2004), urotoxin is selective for hKv1.2 over hKv1.1 and hKv1.3 channels. Due to its unique binding geometry to K^+ channels (see below), whether urotoxin inhibits the toxin-resistant hKv1.5 channel was also tested. Fig. 6D shows that 10 nM urotoxin does not inhibit the hKv1.5 channel (RF = 1.0, SEM = 0.003, N = 5).

Finally, the blocking potency of urotoxin was tested on hKCa3.1 channels for two reasons. First, several peptides which inhibit Kv1.2 also block this channel, such as maurotoxin (Regaya et al., 2004; Wulff and Castle, 2010) and charybdotoxin (Grissmer et al., 1994). Second, urotoxin inhibits hKv1.3, and the selectivity of a peptide for hKv1.3 over the other K^+ channel of human T cells, hKCa3.1, is of great interest due to the potential therapeutic application of these peptides.

Molecular Pharmacology Fast Forward. Published on April 10, 2014 as DOI: 10.1124/mol.113.090183
This article has not been copyedited and formatted. The final version may differ from this version.

Fig. 6A shows that urotoxin inhibits the hKCa3.1 current with a lower potency than charybdotoxin (ChTx), the latter peptide was used as a positive control during the recording of the hKCa3.1 current in HEK cells using a pipette-filling solution allowing full activation of the channels (see Materials and Methods). Fig. 6B shows that 10 nM urotoxin reversibly inhibits the hKCa3.1 current. The Lineweaver-Burk analysis (Fig. 6C) resulted in an IC_{50} = 70 nM which is two orders of magnitude higher than the IC_{50} value for hKv1.2, confirming the preference of urotoxin for the hKv1.2 channel, and indicating similar potential of the toxin for inhibiting hKv1.3 and hKCa3.1 channels.

Analyzing the kinetics of the development and the relief of the inhibition equilibrium we could determine the Kd values of urotoxin for hKv1.1, hKv1.2 and hKCa3.1 channels according to the following formula: Kd = k_{off}/k_{on}, where $k_{off} = (T_{OFF})^{-1}$, $k_{on} = ((T_{ON})^{-1} - (T_{OFF})^{-1})/[Tx]$, [Tx] is the toxin concentration, T_{OFF} and T_{ON} are the time constants for the development and relief of the inhibition at a given toxin concentration (Goldstein and Miller, 1993), respectively. For further details see Supplemental Data (Supplemental Figure 7). The calculated Kd values were 468 nM, 190 pM and 109 nM for hKv1.1, hKv1.2 and hKCa3.1 channels, respectively, in good agreement with the IC_{50} values obtained from the inhibition equilibrium. For Kv1.3 the kinetics of association and dissociation of urotoxin were too fast to be resolved due to the inherent properties of Kv1.3 (i.e., cumulative inactivation).

3.4 Modeling of the 3-D structure of urotoxin

Urotoxin shares high sequence similarity with the α-KTx-6 subfamily of scorpion toxins. Maurotoxin (α-KTx 6.2) and spinoxin (α-KTx 6.13) are known members of this subfamily with which urotoxin shares 50% and 57.9% identity, respectively (Fig. 7). The 3D solution structures of maurotoxin and spinoxin are known (Kharrat et al., 1996; Kobayashi K. et al., 2003), of these, spinoxin was chosen to make the homology modeling of urotoxin. Schrödinger's Maestro software was used for this purpose. Urotoxin is 37 residues long, although it contains 3 more amino acid residues than spinoxin (two at the beginning and one more at the end), but the cysteines are conserved in corresponding positions (Fig. 7). Figure 8 shows the modeled tertiary structure of urotoxin. It has one alpha-helix (residue T8-T19) and two beta-sheets (residues S24-C26, and Y31-C33 respectively). Residues G1-I3 are random coil

Molecular Pharmacology Fast Forward. Published on April 10, 2014 as DOI: 10.1124/mol.113.090183
This article has not been copyedited and formatted. The final version may differ from this version.

(grey); K4 is an isolated bridge (ochre); C5-G7 turn (blue-green); T8-T19 α-helix (purple); T20 coil (grey); C21-N23 Turn (blue-green); S24-C26 β-sheet (yellow); M27-G29 turn (blue-green); K30 isolated bridge (ochre); C31-C33 β-sheet (yellow); Y34-C36 3-10-helix (blue) and V37 unarranged or coil (grey). The best fitting for the homology model was obtained with disulfide bridges between C5-C26, C11-C31, C15-C21 and C33-C36, which resembles the cysteine pairing pattern of maurotoxin (C3-C24; C9-C29; C13-C19; C31-C34 (Kharrat et al., 1996; Kharrat et al., 1997; Rochat et al., 1998)).

Intensive work was performed for the experimental determination of the disulfide pairing of urotoxin. Unfortunately the native toxin was extremely resistant to proteolytic digestion, a condition necessary to open the folded structure and produce peptide fragments that would facilitate identification of the disulfide arrangement. Several aliquots of native urotoxin were separately treated for digestion with trypsin, a mixture of trypsin and chymotrypsin, and both enzymes in the presence of low amounts of solvent (acetonitrile) for 24 hours, at 37 ºC. Selective reduction was also performed before proteolytic digestion, but then the fragments obtained were not sufficiently clear to obtain the disulfide pairing.

3.5. Molecular dynamics simulations

3.5.1 Binding of urotoxin to the hKv1.2 channel

From MD simulation the key residues required for binding to the hKv1.2 channel were identified (Data Supplement hKv1.2). The average position of the toxin throughout the simulation is above the pore possibly preventing the ion conduction (Fig. 9). The toxin binds to the channel mainly in the turret region and in fewer occasions in the pore domain through lysines (K) and arginine (R) interacting strongly with the acidic residues aspartate (D) and glutamate (E) of the channel.

(Supplemental Figure 2) shows the bound state of the toxin-channel complex. Some of the most recurrent toxin-channel residue pairs that form H-bonds are shown in (Supplemental Figure 3). In detail, (Supplemental Figure 3A) shows urotoxin bound to the channel through K17 forming H-bonds with D363 and D379 at the same time; in fact, it is forming a hydrogen network with one residue of the pore region and the other one from the extended turret region. (Supplemental Figure 3B) shows another example of binding throughout the simulation where K17-E355 are forming an H-bond,

Molecular Pharmacology Fast Forward. Published on April 10, 2014 as DOI: 10.1124/mol.113.090183
This article has not been copyedited and formatted. The final version may differ from this version.

whereas on the other end of urotoxin's alpha-helix, at the same time, R9 forms an H-network with D363 and D379. These bindings occur on one side, in the turret region and on the other side, in the pore helix of the channel. The interaction of K17 and E355 is dynamic, the H bond forms and breaks during the whole simulation, thereby allowing K17 to form an H-network with D363 and D379 as well. Another frequent residue pair that was observed is K30-E353 and K16-D379. These H-bonds also form and break during the simulation, indicating the active nature of the toxin-channel interaction. In all cases, the toxin residues were found to act as hydrogen donors.

The results suggest that the toxin maximizes its electrostatic interactions with the peripheral acidic residues of the channel. Data are in agreement with the surface representation of the toxin and channel showing the toxin in blue (positive) and the channel in red (negative) electrostatically predisposed to interact (Supplemental Figure 4). The net charge of the hKv1.2 channel surface is -16 whereas that of urotoxin is +7. It is important to remember that this MD simulation uses brute force dynamics instead of docking, thus the toxin and the channel conserve their flexibility and are free to move during the simulation.

Analysis of the toxin-channel interactions shown above reveals that the toxin binds to the channel primarily, but not exclusively, via two types of basic residues, lysines (positions 16, 17 and 30) and one arginine (position 9) to glutamate and aspartate in the channel.

The lysine residue at position 25 in urotoxin (or position 23 in spinoxin and maurotoxin, as well as in certain other toxins) is conserved across all α-KTx-6 scorpion toxins. Several theoretical docking studies have suggested that this lysine residue protrudes into the channel selectivity filter (Chen and Chung, 2012; Chen et al., 2011; Yi et al., 2008), but in this case, K16, K17 and R9 were the most active residues followed by K30, K25, K32 and K4 in forming hydrogen bonds with E355, E353 and D379 and D363 in the turret and pore helix region, respectively (Supplemental Table 1). A hydrogen bond is considered formed if the donor and acceptor atoms (nitrogen or oxygen) are within 3.2 Å of each other.

Molecular Pharmacology Fast Forward. Published on April 10, 2014 as DOI: 10.1124/mol.113.090183
This article has not been copyedited and formatted. The final version may differ from this version.

All the lysines and arginine-9 in the toxin form salt bridges with D363, D379, E353 and E355. K25 forms a salt bridge only with E355 or E353 (Supplemental Table 2). A salt bridge is considered formed if the distance is less than 3.2 Å between a side chain oxygen atom from an acidic residue and a nitrogen atom from a basic residue.

3.5.2 MD simulation of the binding of urotoxin to the hKv1.1 channel

During the 500 ns simulation (Data Supplement hKv1.1), K25 and K30 from urotoxin were the most common residues involved in forming hydrogen bonds and salt bridges with D377, E351 and E353 of hKv1.1, none of these residues are in the pore helix domain. Other residues involved in the binding were K4, K16, and R9 from the toxin and D377, Y375 and Y379 from the channel (Supplemental Figure 5; Supplemental Tables 3 and 4). These bonds alternate during the simulation. Based on the above, an apparently weaker interaction of urotoxin is predicted with the hKv1.1 channel as compared to the hKv1.2 channel (5 times less bonds), which agrees well with the experimental data where a higher affinity binding of urotoxin to hKv1.2 was observed (see Figs. 4 and 5).

3.5.3 Binding of mutant urotoxin (Lys25Ala) to hKv1.1 and hKv1.2

As mentioned before, within the α-KTx subfamily, K23 has been pointed out as a key residue for the binding of the toxin to Shaker channels. Since the MD results presented above indicated that Lys25 of urotoxin (equivalent to Lys23 in other toxins) is not the key residue for binding to the channel, we decided to run an MD simulation with a mutant urotoxin that lacks K25 (urotoxin-K25A) (Data Supplement hKv1.2_Ala and hKv1.1_Ala) to assess the validity of our brute force dynamic simulation and the role of K25 in the binding.

The results after 500 ns of simulation showed that urotoxin-K25A still binds to hKv1.1 and hKv1.2 channels. Even more, the binding seems to be stronger with this mutant-urotoxin than with native urotoxin (based on the number of bonds made during the simulation). In addition, the binding of the mutant urotoxin involved the same residues as with native urotoxin (all the remaining Ks and R9 from urotoxin binding with the acidic residues in the channel). Therefore, K25 in urotoxin is not the key

Molecular Pharmacology Fast Forward. Published on April 10, 2014 as DOI: 10.1124/mol.113.090183
This article has not been copyedited and formatted. The final version may differ from this version.

residue for its binding to hKv1.1 and hKv1.2 channels and our simulations can be considered accurate (see Supplemental Figure 6).

Molecular Pharmacology Fast Forward. Published on April 10, 2014 as DOI: 10.1124/mol.113.090183
This article has not been copyedited and formatted. The final version may differ from this version.

Discussion

This work describes the isolation and characterization of a K^+ channel blocker toxin, urotoxin, from the venom of the Australian scorpion *Urodacus yaschenkoi*. Urotoxin is a selective and potent blocker of the hKv1.2 channel (IC_{50} = 160 pM); it also blocks hKv1.1, hKv1.3 and hKCa3.1 channels with at least 400-fold lower potency, but it does not inhibit other channels examined in this study.

Comparison of its sequence – 37 amino acids including 8 cysteine residues and C-terminal amidation – with others in the literature shows it belongs to the α–KTx-6 family (Tytgat et al., 1999). The systematic number proposed for urotoxin is α-KTx 6.21 and its assigned Genbank accession number is KC818423. This subfamily consists of a cysteine-stabilized α/β-scaffold that comprises an α-helix connected to a double-stranded β-sheet. So far, the α-KTx-6 subfamily is represented by 4 different scorpion families but has not yet been found in the venom of Buthidae scorpions; urotoxin is the first example from an Urodacidae scorpion.

Based on sequence identity, the closest peptides to urotoxin in the α-KTx-6 subfamily are OcKTx5, OcKTx4 and spinoxin. α-KTx-6 peptides from *O. carinatus* (OcKTx) have not been electrophysiologically characterized; however the predicted structure for these toxins shows the last residue amidated as with urotoxin. OcKTx4 is the only member of the OcKTx family that does not have an amidated C-terminal, probably because it lacks the G at the last position, which is important for amidation of the previous residue (Zhu et al., 2004).

Peptides with ~50-60% identity to urotoxin – Pi-1, Pi-4, hemitoxin and maurotoxin – all inhibit rat Kv1.2 channels with high affinity ranging from IC_{50} = 8 pM to 16 nM (M'Barek et al., 2003; Mouhat et al., 2004; Rochat et al., 1998; Srairi-Abid et al., 2008). Pi-4 has no effect on rat Kv1.1 and Kv1.3 channels but a small effect is observed in rat Ca^{2+}-activated (SK channel) K^+ channels; though the highest affinity for Pi-4 was towards rat Kv1.2 (M'Barek et al., 2003). Pi-1 inhibits the voltage-gated K^+ channel of human T lymphocytes, Kv1.3, with nanomolar affinity (IC_{50} 11 nM) (Peter et al., 1998) and competes with ^{125}I-apamin binding to SK channels in rat brain synaptosomes with an IC_{50} of 50 pM (Mouhat et al., 2004). Maurotoxin, similarly to Pi-1, also inhibits Kv1.3, but also blocks rat Kv1.1

Molecular Pharmacology Fast Forward. Published on April 10, 2014 as DOI: 10.1124/mol.113.090183
This article has not been copyedited and formatted. The final version may differ from this version.

and the Ca^{2+}-activated K^+ channels IKCa1 (KCa3.1) of human T cells (Rochat et al., 1998). Another peptide in the α-KTx-6 subfamily which inhibits Kv1.2 with nanomolar affinity is anuroctoxin (IC_{50} 5 nM) (Bagdany et al., 2005). Anuroctoxin has the lowest identity score to urotoxin and also inhibits Kv1.3 with sub-nanomolar affinity. Thus, considering the pharmacological profile of α-KTx-6 toxins, urotoxin and maurotoxin share a similar pattern of ion channel inhibition, except that urotoxin is particularly selective for Kv1.2 channel.

The 3D structure of urotoxin was predicted based on homology modeling using the solution structure of spinoxin. The 3D model of urotoxin shows the α/β scaffold with one α-helix and two β-sheets bound by four disulfide bridges with the following proposed connectivity: 5-26, 11-31, 15-21, 33-36. The β-sheets in urotoxin, spinoxin and maurotoxin are highly conserved (Table 1) and each has the K23 or K25 positioned properly to form part of the functional dyad required for bioactivity, complemented with the CYGC at the C-termini to provide the aromatic residue for dyad formation. Furthermore, these three toxins have the C-termini amidated. Three amino acids (R14, K15 and G33) were reported to be responsible for the nonconventional pairing of the disulfide bridges in maurotoxin (Kharrat et al., 1997). The amino acids in equivalent positions in urotoxin are K16, K17 and G35, which support the validity of the 3D model and the cysteine pairing of urotoxin proposed in this paper. Nonetheless, it would be desirable to confirm experimentally disulfide bridge pattern of urotoxin. The need for experimental confirmation is underlined by the discrepancy of the 3D model of hemitoxin, which suggested an unusual disulfide bridging pattern, and the experimental data that showed a conventional one (Srairi-Abid et al., 2008). The nonconventional disulfide pairing seems to be important for high affinity binding of maurotoxin to rat Kv1.2 channels. Rendering the disulfide pattern to a conventional one (C1-C5; C2-C6; C3-C7; C4-C8, Pi-1-like) reduced its affinity for Kv1.2 by a factor of ~46 and simultaneously increased its affinity for Shaker B channels by one order of magnitude (M'Barek et al., 2003).

The 3D folding, although important for the high stability of the peptide, does not correlate directly with a specific target molecule (Rodríguez de la Vega et al., 2003). Even though maurotoxin, spinoxin and urotoxin share high sequence and 3D folding similarities, their affinities appear to be different

Molecular Pharmacology Fast Forward. Published on April 10, 2014 as DOI: 10.1124/mol.113.090183
This article has not been copyedited and formatted. The final version may differ from this version.

towards ion channels (Table 2). For example maurotoxin and urotoxin both inhibit Kv1.1, Kv1.2 and Kv1.3 channels, but the affinity of urotoxin for Kv1.2 is at least two orders of magnitude higher than for the other two channels. In contrast, maurotoxin inhibits Kv1.1, Kv1.2 and Kv1.3 channels with a smaller degree of selectivity. Specificity for a given channel requires a minimum a 100-fold difference in IC_{50} (Giangiacomo et al., 2004). This criterion is only fulfilled by urotoxin (ratio IC_{50}Kv1.3/IC_{50}Kv1.2 = 562, for IC_{50}Kv 1.1/IC_{50}Kv1.2 = 1579 and for IC_{50}KCa3.1/IC_{50}Kv1.2 = 435). In contrast, for maurotoxin the ratio is IC_{50}Kv1.1/IC_{50}Kv1.2 = 56, and IC_{50}Kv1.3/IC_{50}Kv1.2 is 225 whereas for spinoxin IC_{50} Kv1.3/IC_{50}Kv1.2 = 25 (Prof. P. Gopalakrishnakone, National University of Singapore, personal communication).

MD simulation is a powerful tool at the molecular level for understanding the electrophysiological experiments performed. The MD simulation shows that residues lysines 16, 17 and 30 and arginine-9 are critical for the blocking of the hKv1.2 channel and the residues involved from the channel are the acidic residues aspartate (363 and 379) and glutamate (355, 353). Urotoxin forms more favorable electrostatic interactions with the outer vestibule of hKv1.2 over hKv1.1, consistent with the selectivity observed experimentally. Our brute force MD simulation results are in agreement with the previous docking models that have been made with αKTx-6 toxins and shaker channels where they state that "*toxins have two to three amino acids that are essential for binding usually arginines or lysines"* (Chen and Chung, 2012; Chen et al., 2011; Visan et al., 2004). To our knowledge, this is the first non-docking simulation made with shaker channels and the longest simulation so far.

Based on *in silico* docking studies, the general inhibitory mechanism of Kv1.2-specific toxins consists of two steps. During the first step a ring of positively charged amino acids (R10, R19, K30 and K33 in Pi4) guide the recognition and correct positioning of the toxin by means of electrostatic interaction with acidic residues in the channel. The subsequent high affinity binding is mediated by hydrophobic forces and hydrogen bonding between the dyad (Y35 in Pi4) and the aromatic cluster of amino acids of the channel (W366, W367, Y377), whereas the dyad lysine protrudes into the selectivity filter and is stabilized there by carbonyl oxygens of the selectivity filter aspartate-379 (M'Barek et al., 2003). Our MD simulation supports strongly the existence of this first step where electrostatic interactions

Molecular Pharmacology Fast Forward. Published on April 10, 2014 as DOI: 10.1124/mol.113.090183
This article has not been copyedited and formatted. The final version may differ from this version.

guide urotoxin to the pore of hKv1.2. In addition, the formation of H-bonds take place involving D379 from the channel and the lysines in the toxin, emphasizing a similar mechanism to other *in silico* docking simulations, however, the final position of the toxin in the pore was beyond the limits of the simulation.

Although the dyad-hypothesis (Dauplais et al., 1997) is suitable to explain the binding of many toxins to the channel pore, high affinity binding of Tc32 to Kv1.3 was also described in the absence of these critical residues in the toxin (Batista et al., 2002). Furthermore, the presence of the functional dyad itself is not a prerequisite for binding of Pi-1 to Kv1.2 (Mouhat et al., 2004), where mutant toxins with substituted dyad residues ([A24, A33]-Pi1) still displayed affinity for Kv1.2. These results allow alternative explanations for the final step of toxin-channel interaction, which may evolve from the position of urotoxin in the pore predicted by the MD simulation (Fig. 9). Nevertheless, the MD simulation with the mutant urotoxin (K25A) supports the accuracy of our simulations as the binding still happens in the absence of K25. This result might suggest that urotoxin would be able to block the hKv1.5 channel as K25 does not make unfavorable interactions with the charged amino acid at the entrance of the pore. The experiment (Fig. 6D) did not confirm this hypothesis. It is important to consider that E355 is missing in Kv1.5 (it is G461 in the equivalent position of Kv1.5), which may explain the lack of inhibition of the hKv1.5 current by urotoxin (please note E355 in Kv1.2 and Kv1.1 is important in urotoxin binding).

Overall, these results demonstrate the potential for urotoxin to become a pharmacological tool to characterize the hKv1.2 channel. Knowledge of the interacting surfaces between the channels and toxins may allow the design of specific drugs to control pathologies associated with K^+ channels such as demyelinating diseases (e.g. Guillian-Barre syndrome, multiple sclerosis) and Lambert-Eaton myasthenic syndrome (Judge and Bever Jr, 2006; Shi and Sun, 2011).

Molecular Pharmacology Fast Forward. Published on April 10, 2014 as DOI: 10.1124/mol.113.090183
This article has not been copyedited and formatted. The final version may differ from this version.

Acknowledgments

The authors also acknowledge M. Sc. Timoteo Olamendi Portugal for amino acid sequence determination, Dr. Cesar Batista and Biol. Erika P. Meneses-Romero at Unidad de Proteomica at IBT, UNAM for molecular mass determination. Authors express gratitude to Dr. Fernando Zamudio for attempting the disulfide bridges connectivity determination.

We would also like to thank Dr. Mike Kupier for giving access to the ANOVA super computer at VLSCI and for his advice.

Molecular Pharmacology Fast Forward. Published on April 10, 2014 as DOI: 10.1124/mol.113.090183
This article has not been copyedited and formatted. The final version may differ from this version.

Authorship Contribution

Participated in research design: Luna-Ramirez, Restano-Cassulini, Bartok, Quintero-Hernandez, Wright, Panyi, and Possani

Conducted experiments: Luna-Ramirez, Bartok, Restano-Cassulini, Coronas, Quintero-Hernandez, and Christensen

Contributed new reagents or analytic tools: Luna-Ramirez, Possani, and Quintero-Hernandez

Performed data analysis: Luna-Ramirez, Restano-Cassulini, Bartok, Quintero-Hernandez, Coronas, Christensen, Panyi, and Possani

Wrote or contributed to the writing of the manuscript: Luna-Ramirez, Quintero-Hernandez, Restano-Cassulini, Bartok, Wright, Panyi and Possani.

Molecular Pharmacology Fast Forward. Published on April 10, 2014 as DOI: 10.1124/mol.113.090183
This article has not been copyedited and formatted. The final version may differ from this version.

References

Bagdany M, Batista CVF, Valdez-Cruz N.A., Somodi S., Rodriguez de la Vega R.C., Licea A.F., Varga Z., Gaspar R., Possani L.D. and G. P (2005) Anuroctoxin, a new scorpion toxin of the alpha-KTx 6 subfamily, is highly selective for Kv1.3 over IKCa1 ion channels of human T lymphocytes. *Mol Pharmacol* **67**: 1034-1044.

Batista C, Gómez-Lagunas F, Rodríguez de la Vega RC, Hajdu P, Panyi G, Gáspár R and LD. P (2002) Two novel toxins from the Amazonian scorpion Tityus cambridgei that block Kv1.3 and Shaker B K($^{+}$)-channels with distinctly different affinities. *Biochim Biophys Acta* **1601**(2): 123-131.

Batista CVF, Román-González SA, Salas-Castillo SP, Zamudio FZ, Gómez-Lagunas F and Possani LD (2007) Proteomic analysis of the venom from the scorpion Tityus stigmurus: Biochemical and physiological comparison with other Tityus species. *Comparative Biochemistry and Physiology - C Toxicology and Pharmacology* **146**(1-2 SPEC. ISS.): 147-157.

Bauer CK and Schwarz JR (2001) Physiology of EAG K+ channels. *Journal of Membrane Biology* **182**(1): 1-15.

Becerril B, Vázquez A, Garcia C, Corona M, Bolivar F and Possam LD (1993) Cloning and characterization of cDNAs that code for Na+ -channel-blocking toxins of the scorpion Centruroides noxius Hoffmann. *Gene* **128**(2): 165-171.

Beraud E, Viola A, Regaya I, Confort-Gouny S, Siaud P, Ibarrola D, Le Fur Y, Barbaria J, Pellissier JF, Sabatier JM, Medina I and Cozzone PJ (2006) Block of neural Kv1.1 potassium channels for neuroinflammatory disease therapy. *Annals of Neurology* **60**(5): 586-596.

Burg ED, Remillard CV and Yuan JXJ (2006) K+ channels in apoptosis. *Journal of Membrane Biology* **209**(1): 3-20.

Chen R and Chung SH (2012) Structural Basis of the Selective Block of Kv1.2 by Maurotoxin from Computer Simulations. *PLoS ONE* **7**(10).

Chen R, Robinson A, Gordon D and Chung SH (2011) Modeling the binding of three toxins to the voltage-gated potassium channel (Kv1.3). *Biophysical Journal* **101**(11): 2652-2660.

Chen X, Wang Q, Ni F and Ma J (2010) Structure of the full-length Shaker potassium channel Kv1.2 by normal-mode-based X-ray crystallographic refinement. *Proc Natl Acad Sci U S A* **107**(25): 11352-11357.

Dauplais M, Lecoq A, Song J, Cotton J, Jamin N, Gilquin B, Roumestand C, Vita C, de Medeiros CL, Rowan EG, Harvey AL and A. M (1997) On the convergent evolution of animal toxins. Conservation of a diad of functional residues in potassium channel-blocking toxins with unrelated structures. *J Biol Chem* **272**(7): 4302-4309.

Gati CDC, Mortari MR and Schwartz EF (2012) Towards therapeutic applications of arthropod venom K +-channel blockers in CNS neurologic diseases involving memory acquisition and storage. *Journal of Toxicology* **2012**.

Giangiacomo KM, Ceralde Y and Mullmann TJ (2004) Molecular basis of α-KTx specificity. *Toxicon* **43**(8): 877-886.

Goldstein SAN and Miller C (1993) Mechanism of charybdotoxin block of a voltage-gated K^+ channel. *Biophysical Journal* **65**(4): 1613-1619.

Goudet C, Chi CW and Tytgat J (2002) An overview of toxins and genes from the venom of the Asian scorpion Buthus martensi Karsch. *Toxicon* **40**(9): 1239-1258.

Grabherr MG, Haas BJ, Yassour M, Levin JZ, Thompson DA, Amit I, Adiconis X, Fan L, Raychowdhury R, Zeng Q, Chen Z, Mauceli E, Hacohen N, Gnirke A, Rhind N, Di Palma F, Birren BW, Nusbaum C, Lindblad-Toh K, Friedman N and Regev A (2011) Full-length transcriptome assembly from RNA-Seq data without a reference genome. *Nature Biotechnology* **29**(7): 644-652.

Grissmer S, Nguyen AN, Aiyar J, Hanson DC, Mather RJ, Gutman GA, Karmilowicz MJ, Auperin DD and Chandy KG (1994) Pharmacological characterization of five cloned voltage-gated K+ channels, types Kv1.1, 1.2, 1.3, 1.5, and 3.1, stably expressed in mammalian cell lines. *Mol Pharmacol* **45**(6): 1227-1234.

Grissmer S, Nguyen AN and Cahalan MD (1993) Calcium activated potassium channels in resting and activated human T lymphocytes: expression levels, calcium dependence, ion selectivity, and pharmacology. . *Journal of General Physiology* **102**: 601-630.

Molecular Pharmacology Fast Forward. Published on April 10, 2014 as DOI: 10.1124/mol.113.090183
This article has not been copyedited and formatted. The final version may differ from this version.

Gurrola GB, Hernández-López RA, Rodríguez De La Vega RC, Varga Z, Batista CVF, Salas-Castillo SP, Panyi G, Del Río-Portilla F and Possani LD (2012) Structure, function, and chemical synthesis of Vaejovis mexicanus peptide 24: A novel potent blocker of Kv1.3 potassium channels of human T lymphocytes. *Biochemistry* **51**(19): 4049-4061.

Huys I, Olamendi-Portugal T, Garcia-Gómez BI, Vandenberghe I, Van Beeumen J, Dyason K, Clynen E, Zhu S, Van Der Walt J, Possani LD and Tytgat J (2004) A subfamily of acidic α-K+ toxins. *J Biol Chem* **279**(4): 2781-2789.

Jouirou B, Mouhat S, Andreotti N, De Waard M and Sabatier JM (2004) Toxin determinants required for interaction with voltage-gated K + channels. *Toxicon* **43**(8): 909-914.

Judge SIV and Bever Jr CT (2006) Potassium channel blockers in multiple sclerosis: Neuronal Kv channels and effects of symptomatic treatment. *Pharmacology and Therapeutics* **111**(1): 224-259.

Kharrat R, Mabrouk K, Crest M, Darbon H, Oughideni R, Martin-Eauclaire MF, Jacquet G, El Ayeb M, Van Rietschoten J, Rochat H and Sabatier JM (1996) Chemical synthesis and characterization of maurotoxin, a short scorpion toxin with four disulfide bridges that acts on K+ channels. *European Journal of Biochemistry* **242**(3): 491-498.

Kharrat R, Mansuelle P, Sampieri F, Crest M, Oughideni R, Van Rietschoten J, Martin-Eauclaire MF, Rochat H and El Ayeb M (1997) Maurotoxin, a four disulfide bridge toxin from Scorpio maurus venom: Purification, structure and action on potassium channels. *FEBS Letters* **406**(3): 284-290.

Kobayashi K., Sugahara Y., Nirthanan S., Huys I., Gopalakrishnakone P, Tytgat J., Sato K. and T K (2003) Three-dimensional solution structure of spinoxin, a potassium channel blocker, PDB.

Legros C, Oughuideni R, Darbon H, Rochat H, Bougis PE and Martin-Eauclaire MF (1996) Characterization of a new peptide from Tityus serrulatus scorpion venom which is a ligand of the apamin-binding site. *FEBS Letters* **390**(1): 81-84.

Luna-Ramírez K, Quintero-Hernández V, Vargas-Jaimes L, Batista CVF, Winkel KD and Possani LD (2013) Characterization of the venom from the Australian scorpion Urodacus yaschenkoi:

Molecular mass analysis of components, cDNA sequences and peptides with antimicrobial activity. *Toxicon* **63**(1): 44-54.

M'Barek S, Mosbah A, Sandoz G, Fajloun Z, Olamendi-Portugal T, Rochat H, Sampieri F, Guijarro JI, Mansuelle P, Delepierre M, De Waard M and JM. S (2003) Synthesis and characterization of Pi4, a scorpion toxin from Pandinus imperator that acts on K+ channels. *Eur J Biochem* **270**(17): 3583-3592.

Martin-Eauclaire MF and Bougis PE (2012) Potassium channels blockers from the venom of Androctonus mauretanicus mauretanicus. *Journal of Toxicology* **2012**.

Mouhat S, Mosbah A, Visan V, Wulff H, Delepierre M, Darbon H, Grissmer S, De Waard M and Sabatier JM (2004) The 'functional' dyad of scorpion toxin Pi1 is not itself a prerequisite for toxin binding to the voltage-gated Kv1.2 potassium channels. *Biochemical Journal* **377**(1): 25-36.

Peter MJ, Varga Z., Panyi G., Bene L., Damjanovich S., Pieri C., Possani L.D. and Jr. GR (1998) Pandinus imperator scorpion venom blocks voltage-gated K+ channels in human lymphocytes. *Biochem Biophys Res Commun* **242**: 621-625.

Possani LD, Becerril B, Delepierre M and Tytgat J (1999) Scorpion toxins specific for Na^+-channels. *European Journal of Biochemistry* **264**(2): 287-300.

Redaelli E, Cassulini RR, Silva DF, Clement H, Schiavon E, Zamudio FZ, Odell G, Arcangeli A, Clare JJ, Alago A, Rodríguez De La Vega RC, Possani LD and Wanke E (2010) Target promiscuity and heterogeneous effects of tarantula venom peptides affecting Na+ and K+ ion channels. *J Biol Chem* **285**(6): 4130-4142.

Regaya I, Beeton C, Ferrat G, Andreotti N, Darbon H, De Waard M and Sabatier J (2004) Evidence for Domain-specific Recognition of SK and Kv Channels by MTX and HsTx1 Scorpion Toxins. *The Journal of Biological Chemistry* **279**(53): 55690.

Restrepo-Angulo I, De Vizcaya-Ruiz A and Camacho J (2010) Ion channels in toxicology. *Journal of applied toxicology : JAT* **30**(6): 497-512.

Robbins CA and Tempel BL (2012) Kv1.1 and Kv1.2: Similar channels, different seizure models. *Epilepsia* **53**(SUPPL. 1): 134-141.

Rochat H, Kharrat R, Sabatier JM, Mansuelle P, Crest M, Martin-Eauclaire MF, Sampieri F, Oughideni R, Mabrouk K, Jacquet G, Van Rietschoten J and El Ayeb M (1998) Maurotoxin, a four disulfide bridges scorpion toxin acting on K+ channels. *Toxicon* **36**(11): 1609-1611.

Rodríguez de la Vega RC, Merino E, Becerril B and Possani LD (2003) Novel interactions between K^+ channels and scorpion toxins. *Trends in Pharmacological Sciences* **24**(5): 222-227.

Rodríguez de la Vega RC and Possani LD (2004) Current views on scorpion toxins specific for K^+-channels. *Toxicon* **43**(8): 865-875.

Shi R and Sun W (2011) Potassium channel blockers as an effective treatment to restore impulse conduction in injured axons. *Neuroscience Bulletin* **27**(1): 36-44.

Shieh CC, Coghlan M, Sullivan JP and Gopalakrishnan M (2000) Potassium channels: molecular defects, diseases, and therapeutic opportunities. *Pharmacological reviews* **52**(4): 557-594.

Srairi-Abid N, Shahbazzadeh D, Chatti I, Mlayah-Bellalouna S, Mejdoub H, Borchani L, Benkhalifa R, Akbari A and El Ayeb M (2008) Hemitoxin, the first potassium channel toxin from the venom of the Iranian scorpion Hemiscorpius lepturus. *FEBS Journal* **275**(18): 4641-4650.

Tan PTJ, Veeramani A, Srinivasan KN, Ranganathan S and Brusic V (2006) SCORPION2: A database for structure-function analysis of scorpion toxins. *Toxicon* **47**(3): 356-363.

Tytgat J, Chandy KG, Garcia ML, Gutman GA, Martin-Eauclaire MF, Van Der Walt JJ and Possani LD (1999) A unified nomenclature for short-chain peptides isolated from scorpion venoms: α-KTx molecular subfamilies. *Trends in Pharmacological Sciences* **20**(11): 444-447.

Visan V, Fajloun Z, Sabatier JM and Grissmer S (2004) Mapping of maurotoxin binding sites on hKv1.2, hKv1.3, and hlKCa1 channels. *Molecular Pharmacology* **66**(5): 1103-1112.

Wang H, Kunkel DO, Schwartzkroin PA and Tempel BL (1994) Localization of Kv1.1 and Kv1.2, two K channel proteins, to synaptic terminals, somata, and dendrites in the mouse brain. *Journal of Neuroscience* **14**(8): 4588-4599.

Wonderlin WF and Strobl JS (1996) Potassium channels, proliferation and G1 progression. *Journal of Membrane Biology* **154**(2): 91-107.

Wulff H and Castle N (2010) Therapeutic potential of KCa3.1 blockers: an overview of recent advances, and promising trends. *Expert Rev Clin Pharmacol* **3**(3): 385-396.

Xie G, Harrison J, Clapcote SJ, Huang Y, Zhang JY, Wang LY and Roder JC (2010) A new Kv1.2 channelopathy underlying cerebellar ataxia. *J Biol Chem* **285**(42): 32160-32173.

Yi H, Qui S, Cao Z, Wu Y and Li W (2008) Molecular basis of inhibitory peptide maurotoxin recognizing Kv1.2 channel explored by ZDOCK and molecular dynamic simulations. *Proteins* **70**: 844-854.

Zhijian C, Feng L, Yingliang W, Xin M and Wenxin L (2006) Genetic mechanisms of scorpion venom peptide diversification. *Toxicon* **47**(3): 348-355.

Zhu S, Huys I, Dyason K, Verdonck F and Tytgat J (2004) Evolutionary Trace Analysis of Scorpion Toxins Specific for K-Channels. *Proteins: Structure, Function and Genetics* **54**(2): 361-370.

Molecular Pharmacology Fast Forward. Published on April 10, 2014 as DOI: 10.1124/mol.113.090183
This article has not been copyedited and formatted. The final version may differ from this version.

11. Footnotes

This work was supported by grants from the Dirección General de Asuntos del Personal Academico, UNAM [IN200113-3]; the Struan Sutherland Fund, AVRU, Dept. of Pharmacology and Therapeutics, The University of Melbourne; scholarship from CONACyT and from The Hugh Williamson Foundation, through Museum Victoria; the European Union and the State of Hungary, co-financed by the European Social Fund in the framework of 'National Excellence Program' [TÁMOP 4.2.4. A/2-11-1-2012-0001] and [TÁMOP 4.2.2-A-11/1/KONV-2012-0025]; and the State of Hungary [OTKA K 75904] and [OTKA NK 101337]. The 3D computer model of urotoxin and the brute force dynamic simulation was supported by a Victorian Life Sciences Computation Initiative (VLSCI) grant number [VR0064] at its Peak Computing Facility at the University of Melbourne, an initiative of the Victorian Government, Australia.

Molecular Pharmacology Fast Forward. Published on April 10, 2014 as DOI: 10.1124/mol.113.090183
This article has not been copyedited and formatted. The final version may differ from this version.

12. Figures Legends

Fig. 1. Purification of urotoxin. HPLC separation of 3 mg soluble venom from *Urodacus yaschenkoi* in a C18 reversed phase column equilibrated with solution A (water in 0.12% TFA), using a gradient from 0 to 60% solution B (acetonitrile in 0.10% TFA) over 60 min. Inset: HPLC repurification of urotoxin (peak marked with an arrow in Fig. 1) was made with a linear gradient of 5-30% of solution B (0.10% TFA in acetonitrile) over 60 min. Asterisk in inset shows pure urotoxin.

Fig. 2. Multiple alignment of urotoxin with similar peptides found in the Next Generation Sequencing analysis. The amino acid sequence of urotoxin was compared with similar sequences resulting from the whole transcriptome analysis made with the Illumina platform. The percentage of identity (% I) between these sequences is shown and for each peptide, the cysteines are highlighted in grey.

Fig. 3. Fraction 4 of the whole venom induced almost complete inhibition of the hKv1.1 voltage-gated K^+ current **(A)**, but has no effect on hKv1.4 **(B)**, hERG1 **(C)** and hELK2 **(D)** K^+ currents. Currents were recorded in the absence (control) or in the presence of 50 µg/ml of Fraction 4 following the block equilibrium (Fraction 4). High potassium extracellular solution was used in hERG1 and hELK2 currents determination. **(A)** The whole-cell hKv1.1 currents were elicited in CHO cells by a voltage pulse to +60 mV (300 ms), followed by a repolarizing step to –50 mV (100 ms) from a holding potential of –90 mV. The time between successive pulses was 2.7 s. (B) The whole-cell hKv1.4 currents were elicited using a similar protocol, by a depolarization step to +40 mV (300 ms) and the time between pulses was 5 s. (C) The whole-cell hERG1 tail currents were recorded in CHO cells at -120 mV (450 ms), preceded by a depolarizing step to +60 mV (500 ms) from a holding potential of –80 mV. The time between successive pulses was 5 s. A 250 ms segment of the inward tail currents is shown for clarity (D) hELK2 currents were evoked by voltage steps to −120 mV for 500 ms from a holding potential of +30 mV. 300 ms segments of the inward tail currents at -120 mV are shown for clarity.

Fig. 4. Block of hKv1.1 current by purified urotoxin. (**A**) Urotoxin blocks hKv1.1 currents expressed in CHO cells. Currents were elicited in a whole-cell patch-clamped cell using depolarizing pulses and

Molecular Pharmacology Fast Forward. Published on April 10, 2014 as DOI: 10.1124/mol.113.090183
This article has not been copyedited and formatted. The final version may differ from this version.

recording conditions as to those described in the legend of Fig. 3. Current traces were recorded in toxin-free solution (control) and at equilibrium block in the presence of urotoxin (1 μM urotoxin). (**B**) Concentration–response relationship curve of urotoxin for hKv1.1 channels. The remaining current fraction (RF, see methods) was determined at various toxin concentrations ($n \geq 3$ independent determinations at each toxin concentration). Data were plotted against concentration and fitted by using a Hill equation giving the following parameters: IC_{50} = 253 nM and H = 1.1. Error bars indicate S.E.M. (**C**) Time course of the development and the relief of the block of macroscopic hKv1.1 currents by urotoxin. The grey bar indicates the application of 1 μM urotoxin. Peak currents were determined from traces shown in panel A during repeated depolarizations and plotted as a function of time.

Fig. 5. Reversible block of hKv1.2 and hKv1.3 currents by 10 nM urotoxin. Urotoxin inhibits hKv1.2, but not hKv1.3, with high affinity. (**A**) The hKv1.2 currents were measured in a voltage-clamped COS7 cell transiently expressing the channel. Currents were evoked by 200 ms long depolarizing pulses from a holding potential of −100 mV to +50 mV every 15 s. (**B**) hKv1.3 currents were recorded in a voltage-clamped activated human peripheral lymphocyte expressing endogenous hKv1.3 channels. The channels were activated by 15 ms depolarization pulses from a holding potential of −100 mV to +50 mV every 15 s. Representative traces show the K^+ currents in the absence (control and wash) and in the presence of 10 nM urotoxin applied in the extracellular bath solution, upon equilibration of the block. **C-D** Time course of the development and the relief of the block of macroscopic hKv1.2 (**C**) and hKv1.3 (**D**) currents by 10 nM urotoxin. Grey bars indicate the perfusion of the recording chamber with 10 nM urotoxin in the bath solution. Peak currents were determined from traces shown in panels A-B during repeated depolarizations (see details in panels A and B) and plotted as a function of time. (**E**) Concentration-response of the inhibition of hKv1.2 channels. Remaining current fraction ($RF = I/I_0$, where I is the peak current in the presence of the toxin in a given concentration, I_0 is the peak current measured in the control solution) is plotted as a function of urotoxin concentration. Peak currents were determined at equilibrium block from experiments shown in panel A. Fitting the Hill equation to the data points yielded IC_{50} = 160 pM and H = 1.1. The error bars indicate the S.E.M. of 3-5 independent measurements. (**F**) The IC_{50} for the hKv1.3 channel was

Molecular Pharmacology Fast Forward. Published on April 10, 2014 as DOI: 10.1124/mol.113.090183
This article has not been copyedited and formatted. The final version may differ from this version.

determined from Lineweaver-Burk analysis, where 1/RF was plotted as a function of toxin concentration and fitting a line to the points, and IC_{50} = 1/slope and H = 1 was used for the Hill equation resulting in IC_{50} = 91 nM on hKv1.3.

Fig. 6. Urotoxin reversibly blocks hKCa3.1 channels with low affinity but does not inhibit hKv1.5. hKCa3.1 or Kv1.5 channels were expressed in tsA201 cells and urotoxin was applied in the bath solution. (**A)** KCa3.1 currents were elicited every 10 s with 150 ms long voltage ramps to +40 mV from −120mV. The holding potential was –100 mV. Representative traces show hKCa3.1 currents in the absence (control and wash) and in the presence of 10 nM urotoxin (as indicated). As a positive control, charybdotoxin (ChTX), a known blocker of hKCa3.1 was used in the same cell (5 nM ChTx). (**B)** Time course of the development and the relief of the block of hKCa3.1 currents by 10 nM urotoxin. The grey bar indicates the application of 10 nM urotoxin in the bath solution. Peak currents were determined at a membrane potential of +40 mV and shown as a function of time. (**C)** The IC_{50} for the hKCa3.1 channel was determined from Lineweaver-Burk analysis (see Materials and Methods) resulting in IC_{50} = 70 nM. (**D)** hKv1.5 currents were elicited by 40 ms long depolarization pulses to +50 mV from a holding potential of -100 mV every 15 s. Representative traces show that 10 nM urotoxin had no effect on hKv1.5. Inset shows the normalized peak currents in the absence and presence (grey bar) of 10 nM urotoxin in the bath solution.

Fig. 7. Multiple alignment of urotoxin with different potassium toxins from scorpions. This alignment shows the percentage of identity, % I, of several potassium toxins with respect to urotoxin. The conserved cysteines are shown in grey (shaded). Amidated residues are shown in bold and underlined. Glycine residues involved in amidation are shaded. OcKTx5: Potassium channel toxin alpha-KTx 6.10 from *Opistophthalmus carinatus;* OcKTx4: Potassium channel toxin alpha-KTx 6.9 from *Opistophthalmus carinatus*; Spinoxin: Potassium channel toxin alpha-KTx 6.13 from *Heterometrus spinifer*; Pi-1: Potassium channel toxin alpha-KTx 6.1 from *Pandinus imperator*; Pi-4: Potassium channel toxin alpha-KTx 6.4 from *Pandinus imperator*; Hemitoxin: Potassium channel toxin alpha-KTx 6.15 from *Hemiscorpius lepturus*; Maurotoxin: Potassium channel toxin alpha-KTx 6.2 from *Scorpio maurus palmatus*; Pi-7: Potassium channel toxin alpha-KTx 6.5 from *Pandinus imperator*;

Molecular Pharmacology Fast Forward. Published on April 10, 2014 as DOI: 10.1124/mol.113.090183
This article has not been copyedited and formatted. The final version may differ from this version.

OcKTx1: Potassium channel toxin alpha-KTx 6.6 from *Opistophthalmus carinatus*; OcKTx2: Potassium channel toxin alpha-KTx 6.7 from *Opistophthalmus carinatus*; OcKTx3: Potassium channel toxin alpha-KTx 6.8 from *Opistophthalmus carinatus*; HsTx1: Potassium channel toxin alpha-KTx 6.3 from *Heterometrus spinifer*; Anuroctoxin: Potassium channel toxin alpha-KTx 6.12 from *Anuroctonus phaiodactylus*. UniProtKB/Swiss-Prot Access number is indicated in parentheses.

Fig. 8. Predicted tertiary structure of urotoxin showing the disulfide bridges. Maestro model visualized with VMD showing New Cartoon drawing method. Toxin starts in the upper grey coil. Residues G1-I3 are unarranged or in coil (grey); K4 is an isolated bridge (ochre); C5-G7 Turn (blue-green); T8-T19 α-helix (purple); T20 coil (grey); C21-N23 Turn (blue-green); S24-C26 β-sheet (yellow); M 27-G29 turn (blue-green); K30 isolated bridge (ochre); C31-C33 β-sheet (yellow); Y34-C36 3-10-helix (blue) and V37 unarranged or coil (grey).

Fig. 9. Average position of urotoxin with respect to hKv1.2 during the MD simulation. Urotoxin is shown in purple near the pore domain. The channel is in grey. Highlighted (in color) are the most active residues forming H-bonds and salt bridges during the 500 ns simulation.

Data Supplement hKv1.2. Molecular dynamics simulation (500ns) of hKv1.2 and urotoxin (pdb file: 'kv12_FINAL').

Data Supplement hKv1.1. Molecular dynamics simulation (500ns) of hKv1.1 and urotoxin (pdb file: 'kv11_FINAL').

Data Supplement hKv1.2_Ala and hKv1.1_Ala. Molecular dynamics simulation (500ns) of hKv1.2 and mutant-urotoxin (pdb file: 'kv12_ALA'). Additionally, the molecular dynamics simulation (500 ns) of hKv1.1 and mutant urotoxin (pdb file: 'kv11_ALA') was performed.

Molecular Pharmacology Fast Forward. Published on April 10, 2014 as DOI: 10.1124/mol.113.090183
This article has not been copyedited and formatted. The final version may differ from this version.

13. Tables

Table 1. Secondary structure of urotoxin, spinoxin and maurotoxin

Toxin	α-helix	β_1-sheet	β_2-sheet
Urotoxin	8-19 T-T	24-26 SKC	31-33 CKC
Spinoxin	10-17 Y-T	22-24 AKC	29-31 CKC
Maurotoxin	6-17 S-T	22-25 AKC	28-31 SKCK

Molecular Pharmacology Fast Forward. Published on April 10, 2014 as DOI: 10.1124/mol.113.090183
This article has not been copyedited and formatted. The final version may differ from this version.

Table 2. Bioactivity comparison of maurotoxin, spinoxin and urotoxin showing IC_{50} values at nM concentrations.

Toxin/Channel	Kv1.1	Kv1.2	Kv1.3	Other
Maurotoxin	45	0.8	180	SK/KCNN and KCa3.1 (1 nM)
Spinoxin	NA	2.5	63	
Urotoxin	253	0.16	91	KCa3.1 (70 nM)

NA = Not active; SK/KCNN = apamin-sensitive small conductance calcium-activated potassium channels; and KCa3.1/KCNN4 = intermediate conductance calcium-activated potassium channels.

Figure 1.

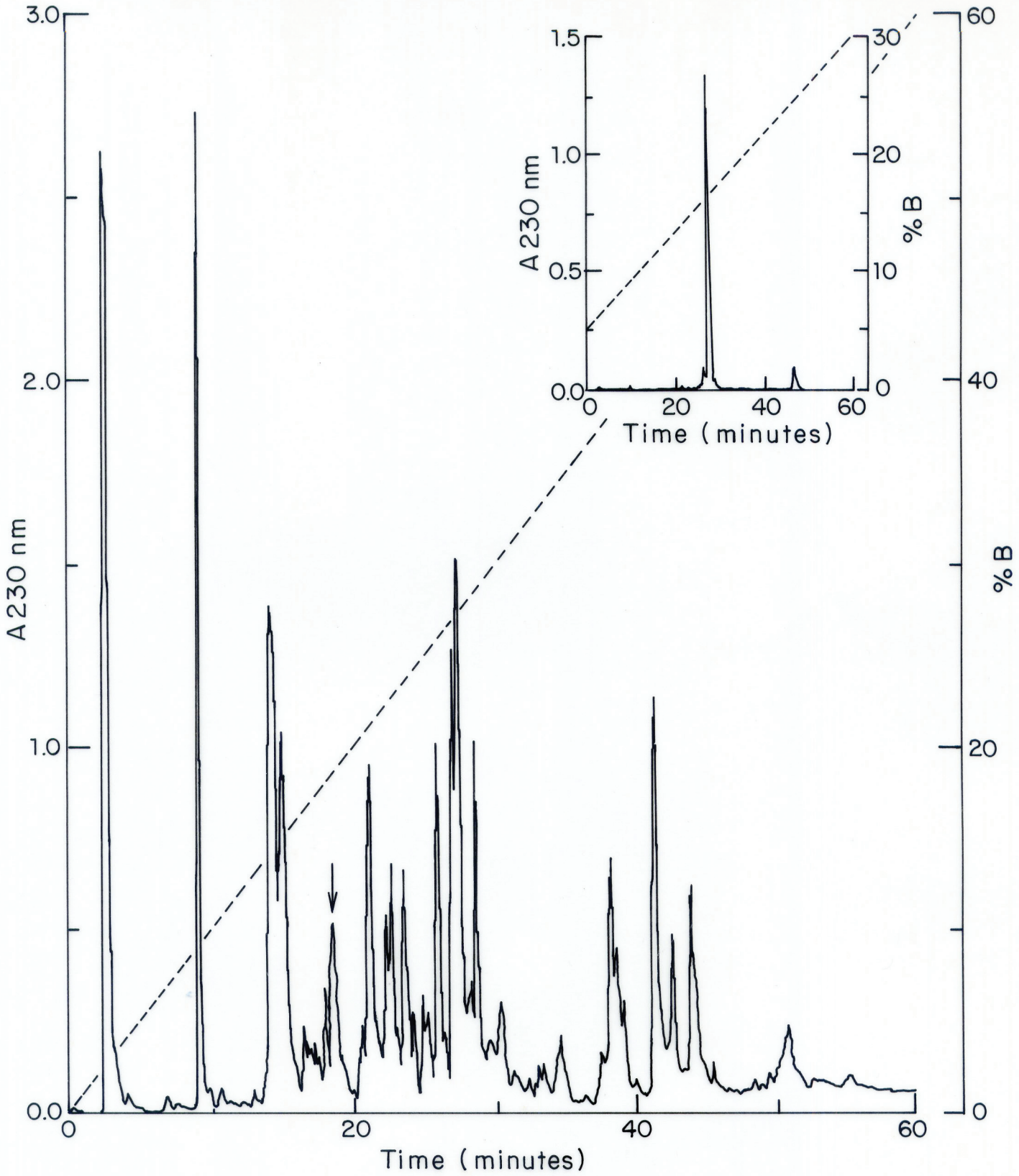

Molecular Pharmacology Fast Forward. Published on April 10, 2014 as DOI: 10.1124/mol.113.090183
This article has not been copyedited and formatted. The final version may differ from this version.

Figure 2.

Figure 3.

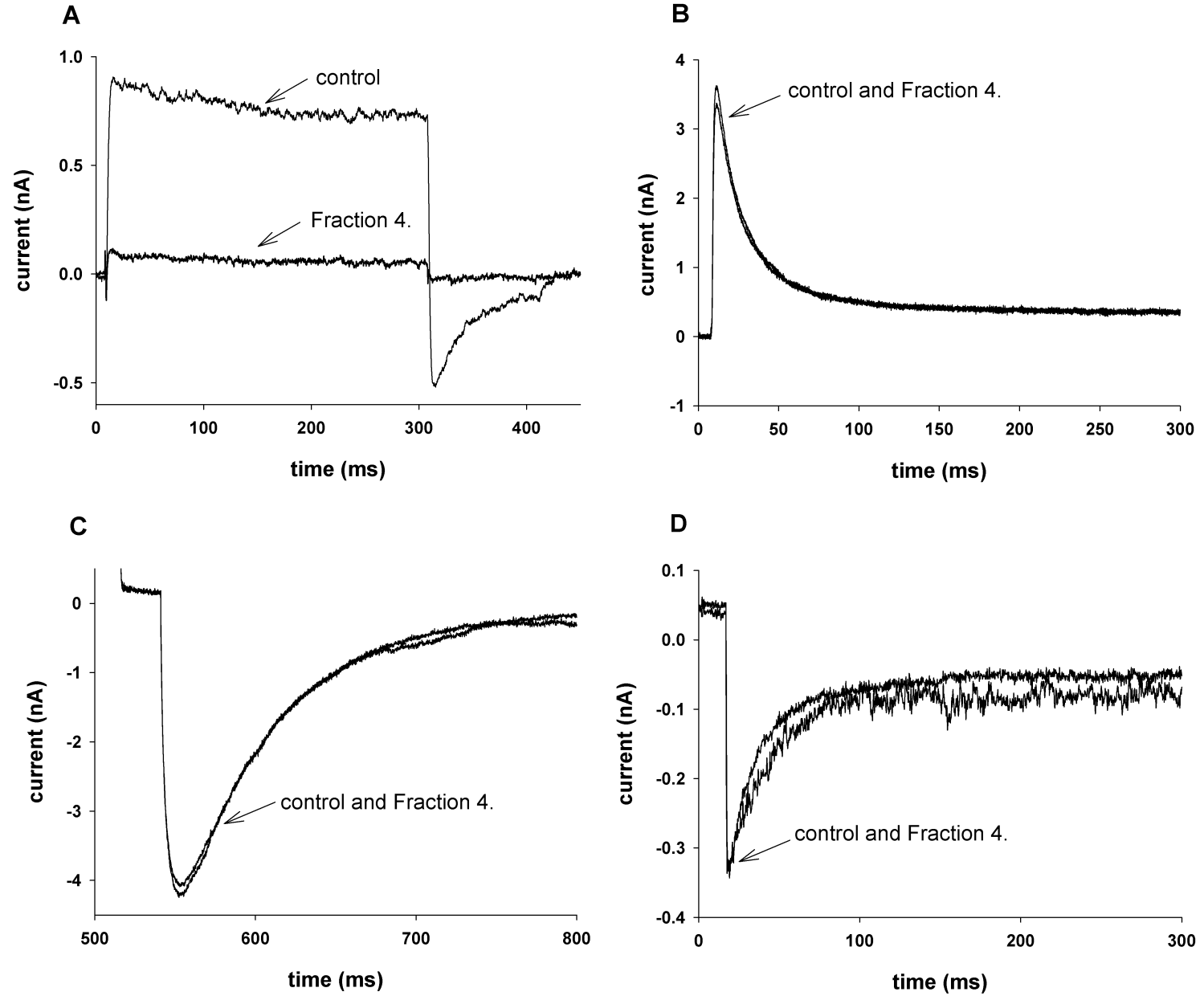
A
1.0
0.5
0.0
-0.5
current (nA)
control
Fraction 4.
0
100
200
300
400
time (ms)
B
4
3
2
1
0
-1
current (nA)
control and Fraction 4.
0
50
100
150
200
250
300
time (ms)
C
0
-1
-2
-3
-4
current (nA)
control and Fraction 4.
500
600
700
800
time (ms)
D
0.1
0.0
-0.1
-0.2
-0.3
-0.4
current (nA)
control and Fraction 4.
0
100
200
300
time (ms)

Figure 4.

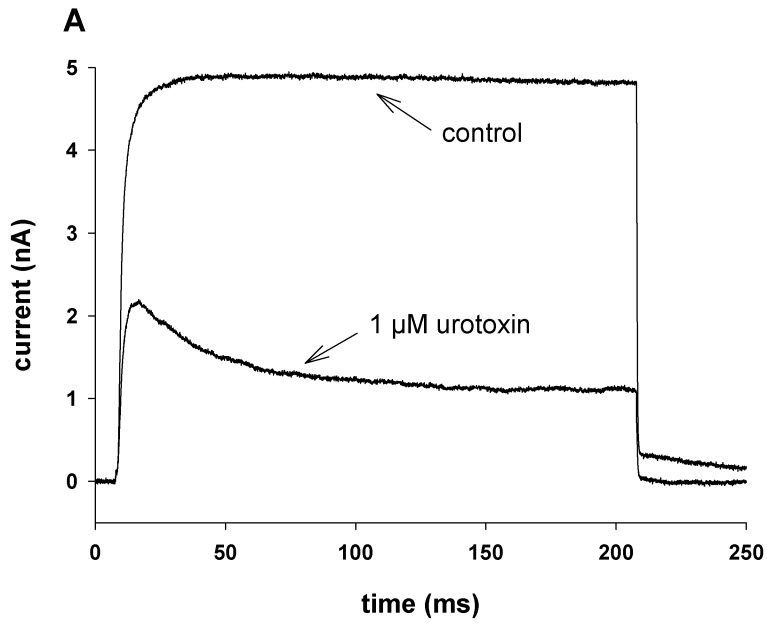
A
control
1 μM urotoxin
current (nA)
time (ms)

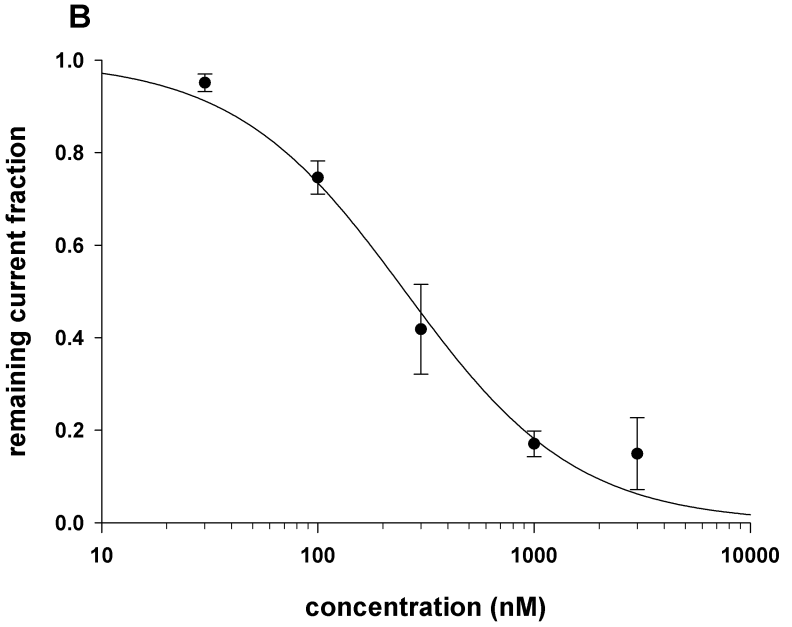
B
remaining current fraction
concentration (nM)

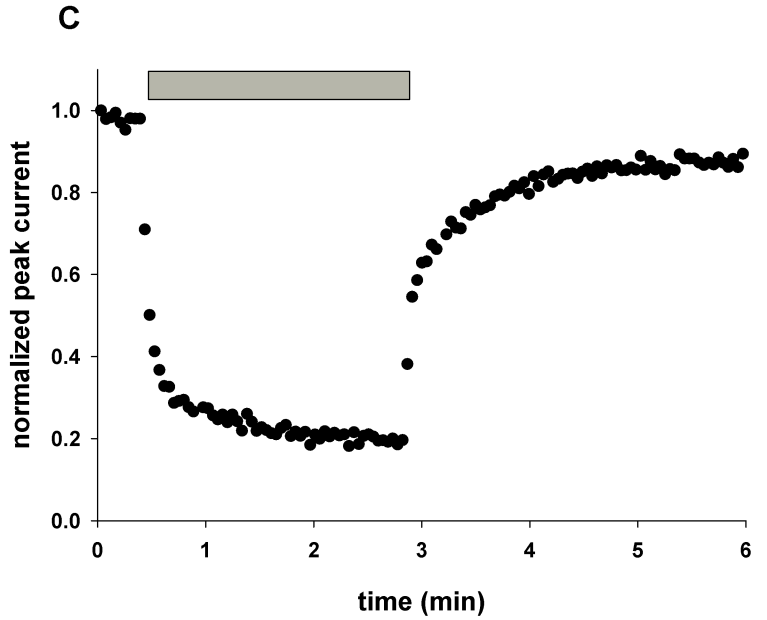
C
normalized peak current
time (min)

Figure 5.

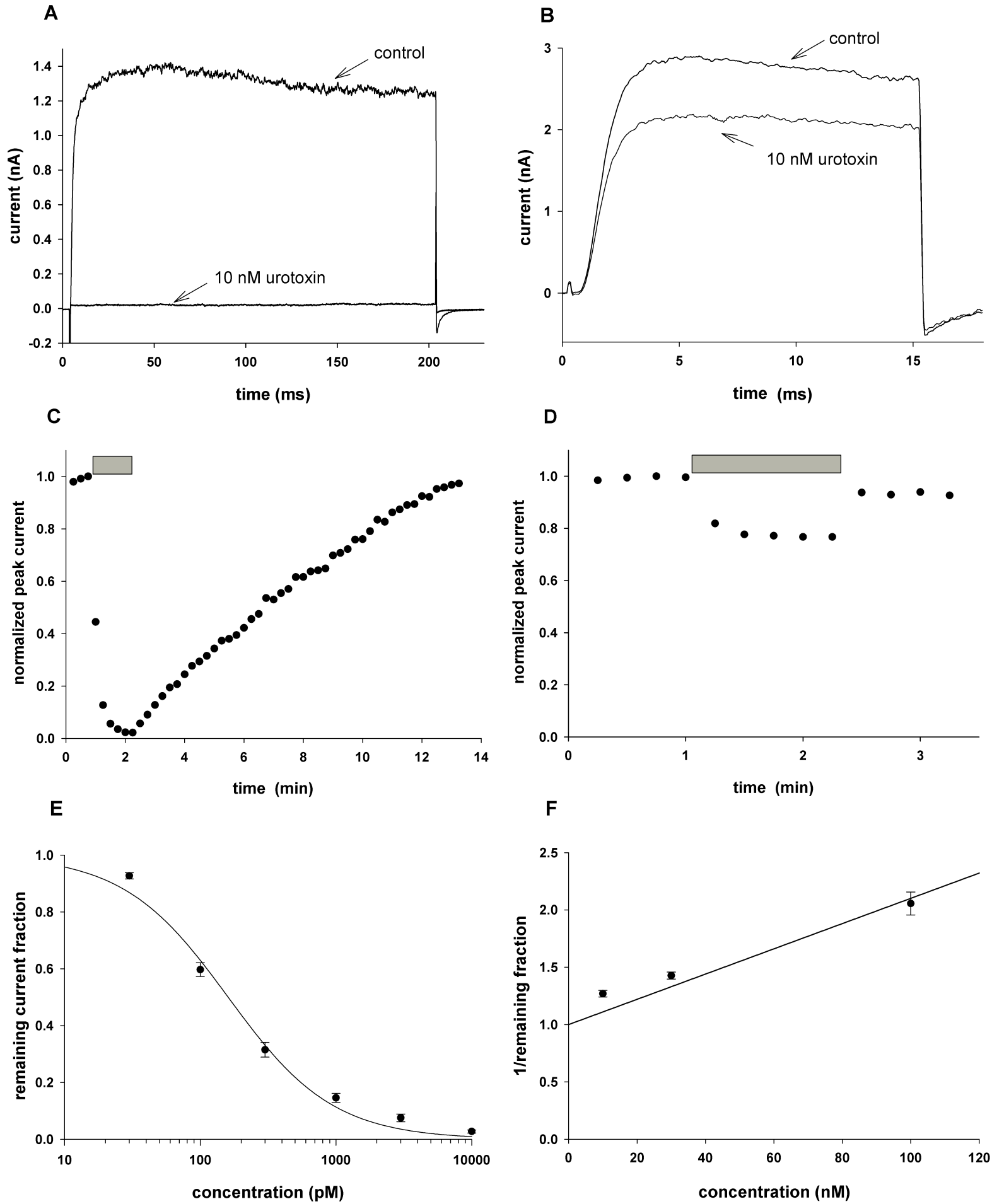

Figure 6.

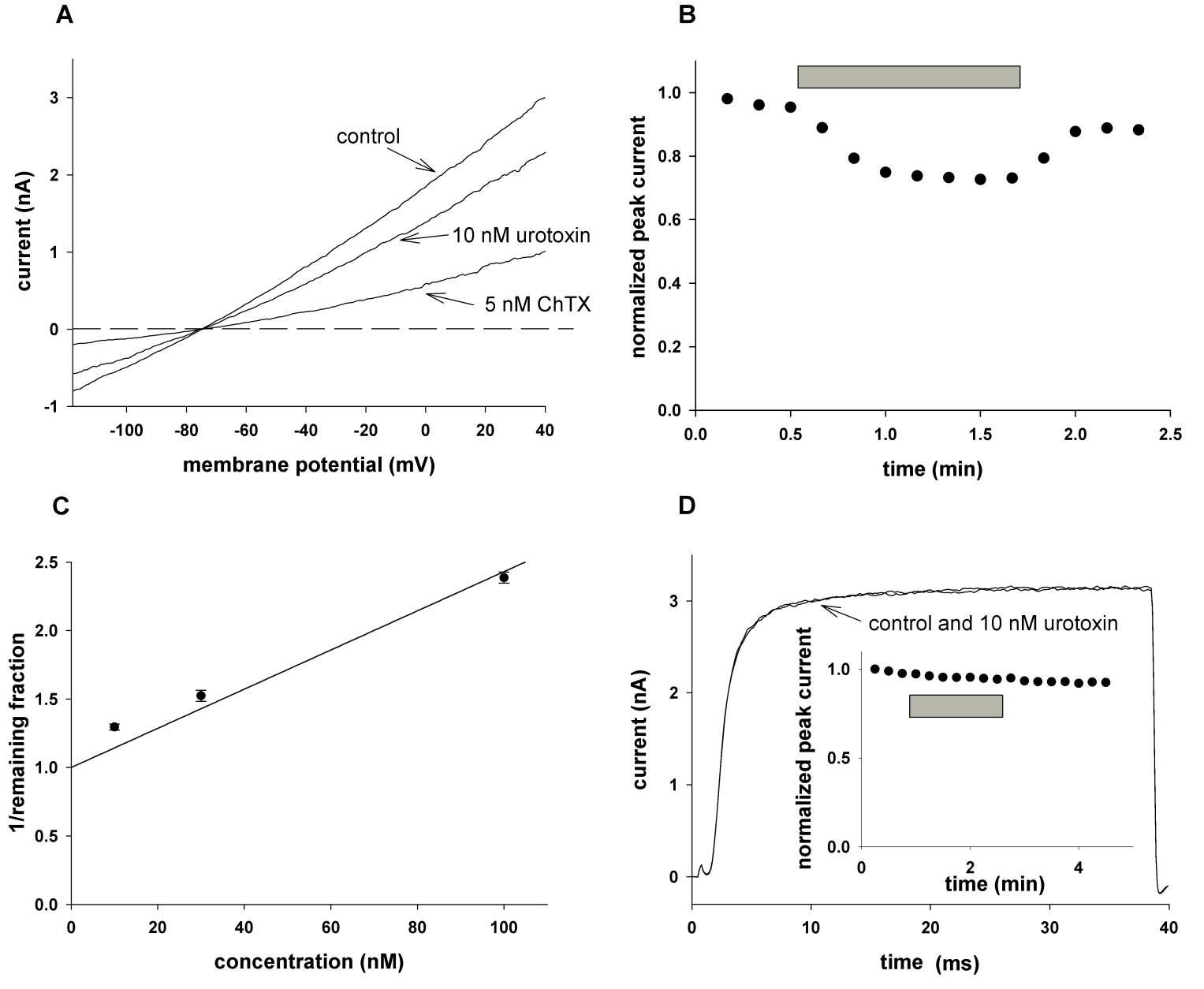
A
control
10 nM urotoxin
5 nM ChTX
current (nA)
membrane potential (mV)
B
normalized peak current
time (min)
C
1/remaining fraction
concentration (nM)
D
control and 10 nM urotoxin
current (nA)
time (ms)
normalized peak current
time (min)

Molecular Pharmacology Fast Forward. Published on April 10, 2014 as DOI: 10.1124/mol.113.090183
This article has not been copyedited and formatted. The final version may differ from this version.

Figure 7.

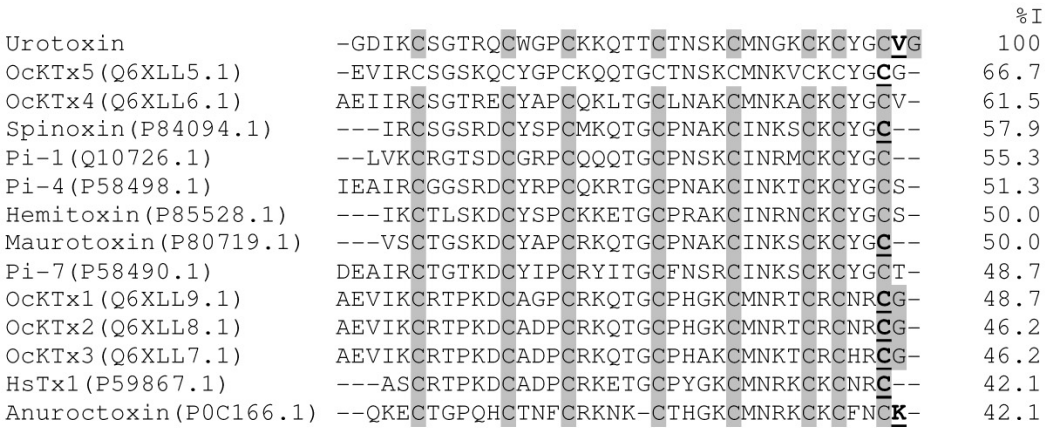

Figure 8.

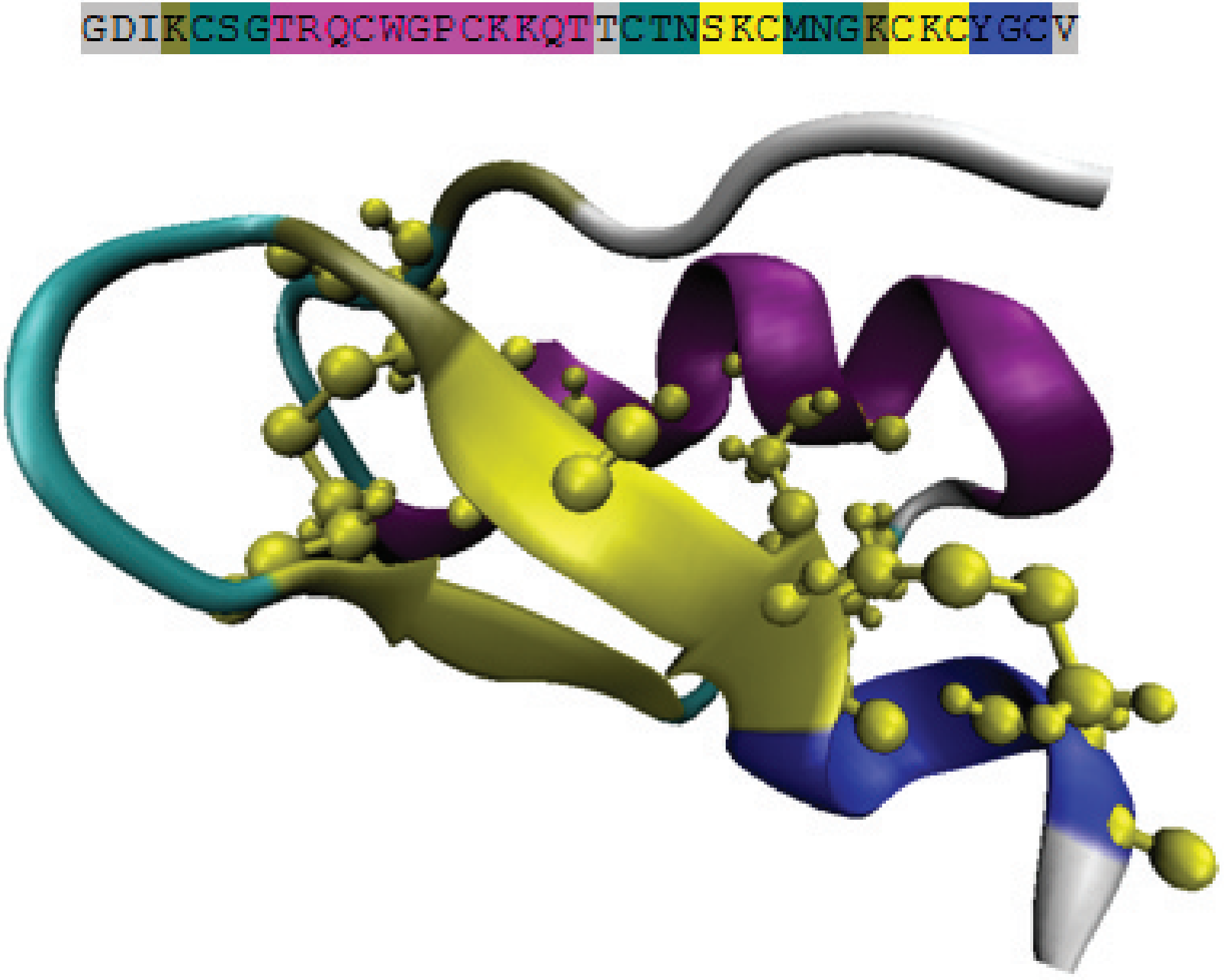

Molecular Pharmacology Fast Forward. Published on April 10, 2014 as DOI: 10.1124/mol.113.090183
This article has not been copyedited and formatted. The final version may differ from this version.

Figure 9.